Crystal field effects on $3d^0$ systems (Ti4+)

$3d^0$ systems in octahedral symmetry

We start with the calculation of the atomic symmetry, but now including the crystal field program, as we did in chapter 1 for Ni2+. The files als4ti4a.rcg and als4ti4a.rac perform this calculation. The file als4ti4a.rcg has the following lines:

```
   10    1    0   14    2    4    1    1 SHELL03000000 SPIN03000000 INTER8
    0                        80998080            8065.47800     0000000
    1     2 1 12 1 10         00      9 00000000 0 8065.4790 .00       1
P 6  S 0
P 5  D 1
Ti4+ 2p06 3d00     1    0.0000    0.0000    0.0000    0.0000    0.0000HR99999999
Ti4+ 2p05 3d01     6  464.8110    3.7762    0.0322    6.3023    4.6284HR99999999
    2.6334
Ti4+ 2p06 3d00      Ti4+ 2p05 3d01        -0.26267( 2P//R1// 3D) 1.000HR  38-100
                    -99999999.
   -1
```

Compared with the original file als3ti4.rcg, some changes have been made in this inputfile with the goal to continue with the crystal field calculation afterwards. The changes one has to make are all in the first line:

```
10    1    0   00    4    4    1    1 SHELL00000000 SPIN00000000 INTER8
10    1    0   14    2    4    1    1 SHELL03000000 SPIN03000000 INTER8
```

The 14 indicates the name of the output file that is used in RAC. It is renamed to als4ti4a.m14. The change to 2 is needed for calculations in low symmetry. It tells the program to calculate the additional matrices (see below). The SHELL comment has its second 0 changed to a 3. This implies that a crystal field can be added on the second shell as defined in the RCG file, which is the 3d-shell. The SPIN comment has also its second 0 changed to a 3. This implies that a magnetic (or exchange) field can be added, again on the second shell. In principle, one can add fields on any shell, but acting on core shells does not make physical sense.

These changes have to be made in all cases where one would like to add a crystal field and/or a magnetic field. The general procedure is to start from a RCN2 calculation and modify the .rcf file according to the procedure given above.

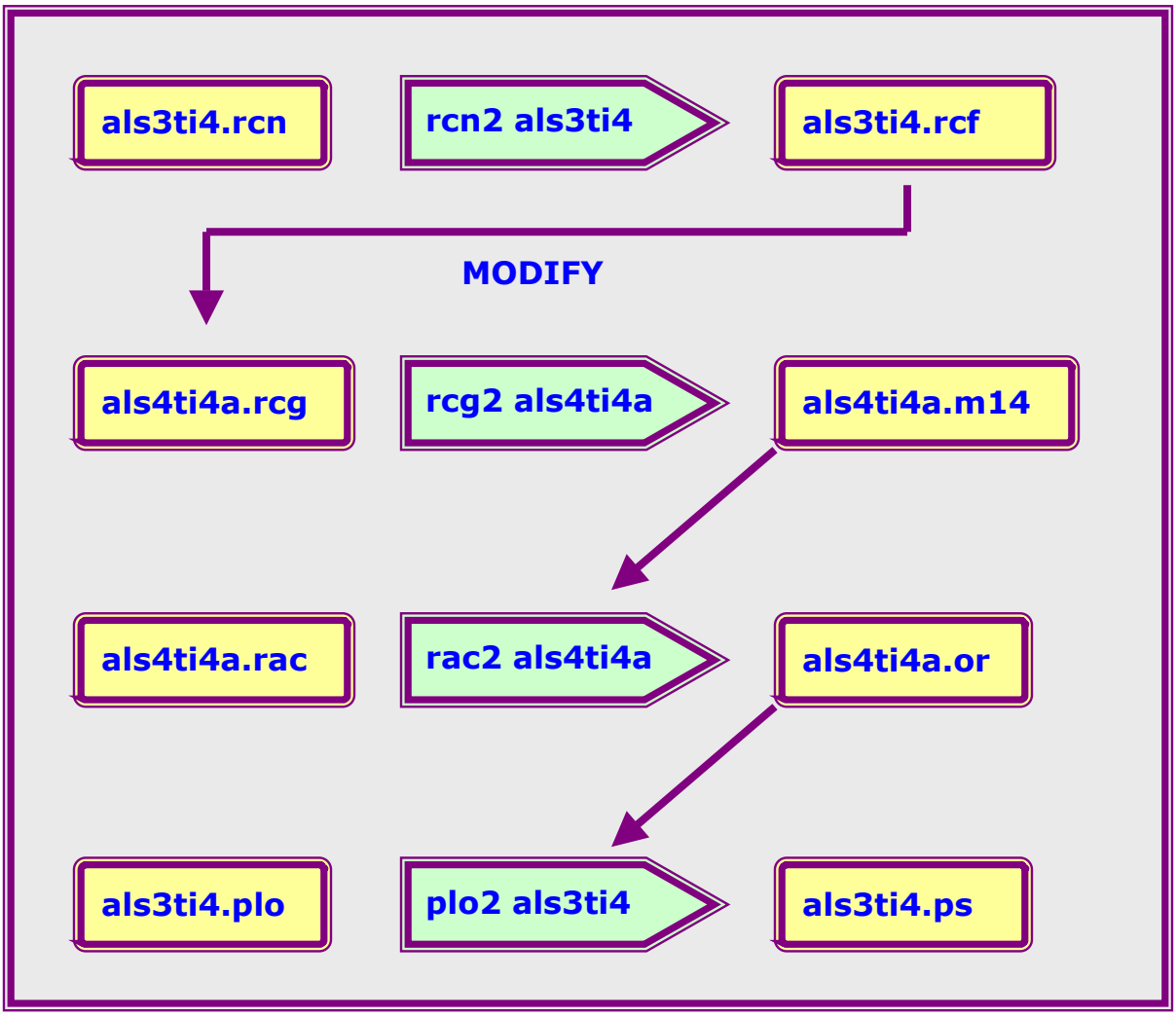

We have performed two sets of crystal field multiplet calculations for Ti4+ ions. The files als4ti4a.rcg and als4ti4.rac recalculate the atomic multiplet spectrum by using a zero value for the crystal field splitting. In chapter 1, we have introduced the structure of the .rac inputfile. It is reproduced below. The values in red are the crystal field strengths in the initial and final state. They are both set to zero.

The files als4ti4b.rcg and als4ti4b.rac calculate the crystal field multiplet spectrum for a crystal field of 2.218 eV. The file als4ti4b.rcg is identical to als4ti4a.rcg. The only change that is made in the file als4ti4b.rac is the change of the crystal field values from 0.0 to 7.0. A value of 7.0 indicates a crystal field of 7.0 * 0.304 = 2.218 eV.

```
Y
    % vertical 1 1
 butler O3
 to    Oh
 endchain
 actor   0+ HAMILTONIAN ground  PRINTEIG
  OPER HAMILTONIAN
    BRANCH 0+ > 0 0+      1.0
  OPER SHELL2
    BRANCH 4+ > 0 0+      0.00
 actor   0+ HAMILTONIAN excite  PRINTEIG
  OPER HAMILTONIAN
    BRANCH 0+ > 0 0+      1.0
  OPER SHELL2
    BRANCH 4+ > 0 0+      0.00
 actor  1- plane       transi PRINTTRANS
   oper MULTIPOLE
     branch  1- > 0 1-   1.000
RUN
```

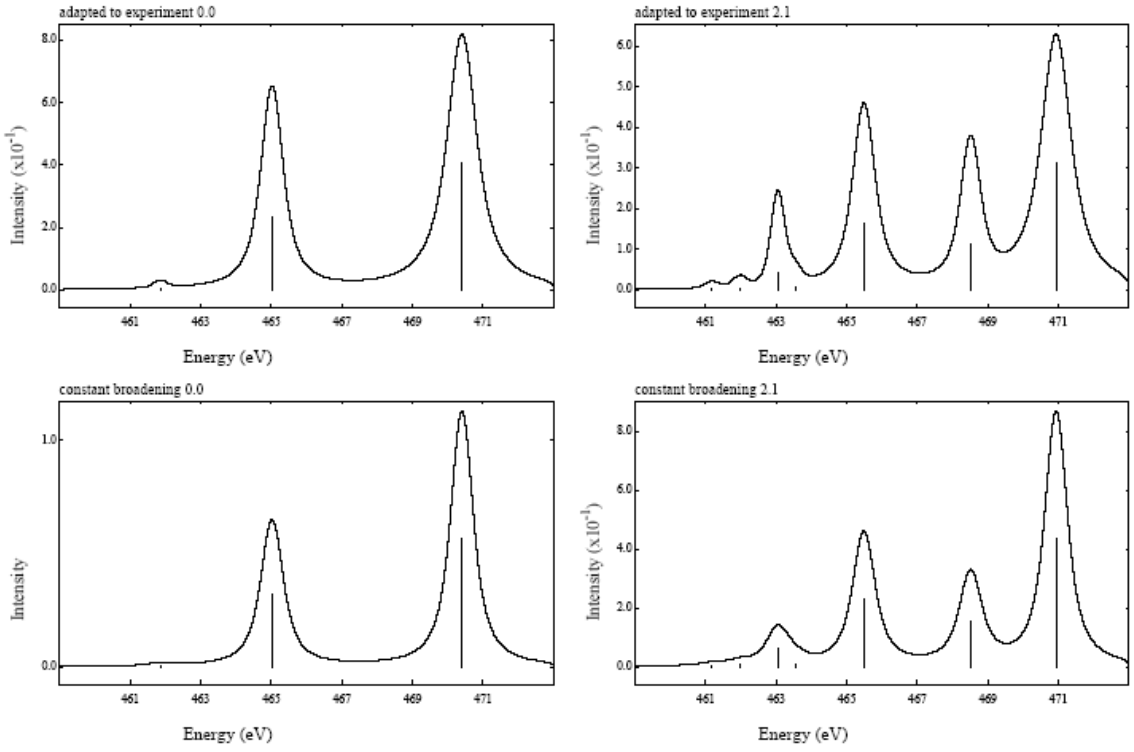

The figure shows the result of the als4ti4a calculation (left) and the als4ti4b calculation (right). The als4ti4a calculation shows the same result as found in chapter 3 for a Ti4+ atom, with three peaks. In the figure we used two different settings for the broadenings. The bottom figure uses a constant broadening, while the top calculation uses a broadening that is different for every peak. In this way, the spectrum can be adapted to the experiment, as it turns out that in experiment there are different

broadenings for different peaks. The als4ti4b calculation shows seven peaks; after broadening the third and fourth peak overlap and one finds six peaks in the spectrum. These seven peaks are given at the bottom of the als4ti4b.ora file.

```
TRANSFORMED MATRIX for TRIAD  2  (  0+   1-   1- 0) (1*7)  DIM :1:3:3   ACTOR
PLANE

       ---- MATRIX ----      PRINTTRANS

 BRA/KET :  461.1850  461.9710  463.0501  463.5387  465.4900  468.5141  470.9370
-------------------------------------------------------------------------------
  0.00000:  0.009445  0.015776  0.137714  0.021110  0.505803  0.346162  0.963990

 TRANSFORMATION FINISHED
```

This part of the als4ti4b.ora file gives the 'transformed matrix for triad2', where 'triad2' is the transition from 0+ via 1- to 1- symmetry. Then follows a matrix with seven energies and seven intensities, which constitutes the complete result from the calculation. These seven sticks are then broadened in the plotting program. The meaning of 'triad2' and the respective symmetries will be explained below. A complication is the notation of the RAC2 program, which uses BUTLER notation, instead of the more familiar SCHONFLIESS notation for group symmetries. The translation between the two notations is given below in the character table of O_h symmetry. Here we note that 0+ identifies with A1g and 1- with T1u, which means that triad2 is the calculation of the transition matrix $<A_{1g}|T_{1u}|T_{1u}>$ in O_h symmetry. The dipole transition has T1u symmetry in an octahedral field.

Crystal Field effects on 3d0 systems

In this section we will focus on the discussion of the crystal field effects on the spectral shape of $3d^0$ systems. The $3d^0$ systems are special because they are not affected by ground state effects. The $3d^0 \rightarrow 2p^5 3d^1$ transition can be calculated from a single transition matrix $<A_1|T_1|T_1>$ in O_h symmetry. The ground state A_1 matrix is 1x1 and the final state T_1 matrix is 7x7, making the transition matrix 1x7. In other words the spectrum consists of a maximum of seven peaks. Chapter 3 showed the complete calculation in SO_3 symmetry. Below the branching from SO3 to Oh symmetry will be explained; for the moment we just use them. The respective degeneracies of the J-values in SO_3 symmetry and the degeneracies of the representations in O_h symmetry are collected in this table.

J in SO_3	Deg.	Branching	Γ in O_h	Deg.
0	1	A_1	A_1	2
1	3	$3\times T_1$	A_2	3
2	4	$4\times E$, $4\times T_2$	T_1	7
3	3	$3\times A_2$, $3\times T_1$, $3\times T_2$	T_2	8
4	1	A_1, E, T_1, T_2	E	5
$\sum$	12			25

It can be seen that a $2p^5 3d^1$ configuration has twelve representations in SO_3 symmetry that are branched to 25 representations in a cubic field. The overall degeneracy of the $2p^5 3d^1$ configuration is 6x10=60, implying a possibility of 60 transitions in a system without any symmetry. From these 25 representations, only seven are of interest for the calculation of the x-ray absorption spectral shape, because only these T_1 symmetry states obtain a finite intensity.

	461.856	462.329	462.613	463.442	465.024	468.588	470.405
1	0.0924	0.0000	0.0000	0.0000	0.6001	0.0000	0.3075
2	0.9009	0.0000	0.0000	0.0000	0.0384	0.0000	0.0607
3	0.0068	0.0000	0.0000	0.0000	0.3615	0.0000	0.6318
4	0.0000	0.0000	0.6019	0.0364	0.0000	0.3617	0.0000
5	0.0000	0.0000	0.0459	0.6674	0.0000	0.2867	0.0000
6	0.0000	0.0000	0.3521	0.2963	0.0000	0.3516	0.0000
7	0.0000	1.0000	0.0000	0.0000	0.0000	0.0000	0.0000
	0.0001	0.0000	0.0000	0.0000	0.2466	0.0000	0.7533

This table shows the seven T_1 symmetry states calculated with a crystal field splitting of 0.0 eV. One finds the three peaks that are related to J=1 final states, build from vector rows one, two and three. The third row is related to the $^1P_1$ state and the intensity of the peak as given in the bottom row is equal to the square of this row, where the total intensity is normalised to 1.0. Rows four, five and six are related to the J=3 states and row seven is related to a J=4 state. It can be seen that with a value of 10Dq of 0.0 eV, the 7x7 matrix blocks out to two 3x3 and one 1x1 matrices because one essentially is calculating a spectrum in SO_3 symmetry.

The T_1 final states of the $2p^5 3d^1$ configuration with 10Dq=3.04 eV. The top row gives the energies and the bottom row the relative intensities of the seven final states that are build from seven basis-vectors.

	460.828	461.641	462.806	464.048	465.859	468.313	471.369
1	0.0662	0.0037	0.1550	0.0124	0.4916	0.0404	0.2308
2	0.5944	0.0253	0.0007	0.2972	0.0280	0.0078	0.0466
3	0.0046	0.0091	0.1128	0.0046	0.1845	0.2666	0.4178
4	0.0161	0.4460	0.0340	0.0980	0.0097	0.2923	0.1039
5	0.0020	0.2973	0.2980	0.0791	0.0331	0.2191	0.0714
6	0.0044	0.0404	0.3986	0.0116	0.2417	0.1738	0.1294
7	0.3124	0.1781	0.0009	0.4972	0.0113	0.0000	0.0001
	0.0001	0.0003	0.0435	0.0001	0.1164	0.2430	0.5968

This table shows the seven T_1 symmetry states calculated with a crystal field splitting of 3.04 eV. One finds the seven peaks that are all build from the seven basis vectors. The third row is again related to $^1P_1$ symmetry and its square yields the intensity as given in the bottom row. Essentially one observes four main peaks, peaks 3, 5, 6 and 7. Peak 6 and 7 are essentially the L_2 edge peaks of respectively t_{2g} and e_g character. They are split by 3.05 eV, essentially the value of 10Dq. Peaks 3 and 5 are the L_3 peaks of t_{2g} and e_g character, also split by 3.05 eV. Peaks 1, 2 and 4 are low-intensity peaks that originate from the 'spin-forbidden transition' in the atomic multiplet calculation.

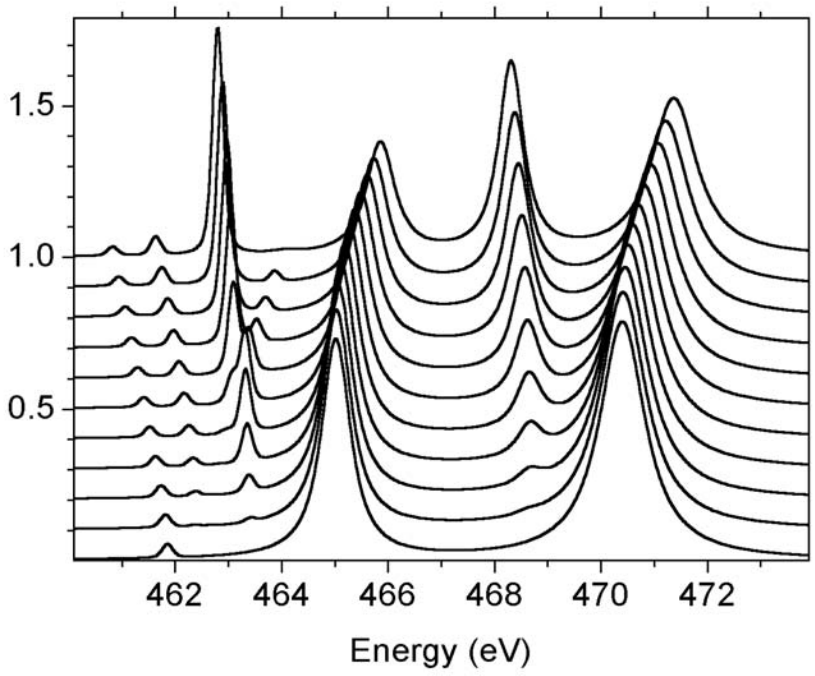

This figure shows the crystal field multiplet calculations for the $3d^0 \rightarrow 2p^5 3d^1$ transition in Ti^{IV}. The result of each calculation is a set of seven energies with seven intensities.

EXERCISE:
1. Try to reproduce this figure by calculating the crystal field multiplet spectrum of Ti4+ as a function of the crystal field strength. The parameter to change is the value of the line "BRANCH 4+ > 0 0+ 0.00". The figure can be reproduced by setting the crystal field strengths from 0.0 to 10.0, in steps of 1.0, which identifies with steps of 0.304 eV.
2. What happens if one changes the initial state crystal field value and the final state crystal field value independently?
3. What happens if one sets the crystal field values to negative numbers?
4. What happens if one uses very large crystal field values, say a value of 100 eV?

The seven states have been broadened by the lifetime broadening and the experimental resolution. From a detailed comparison to experiment it turns out to be the case that each of the four main lines has to be broadened differently. It is well known that the L_2 part of the spectrum (i.e. the last two peaks) contains an additional Auger decay that accounts for a significant broadening with respect to the L_3 part. This effect has been found to be an additional broadening of 0.5 eV half-width half-maximum. For more details see degroot90a.pdf. An additional difference in broadening is found between the t_{2g} and the e_g states. This broadening has been ascribed to differences in the vibrational effects on the t_{2g} respectively the e_g states. Another cause could be a difference in hybridisation effects and in fact charge transfer multiplet calculations indicate that this effect is more important than vibrational effects, as was shown in okada93a.pdf. Whatever the origin of the broadening, the comparison with experiment shows that if one performs crystal field multiplet calculations, the e_g states must be broadened with an additional 0.4 eV hwhm for the Lorentzian parameter. The experimental resolution has been simulated with a Gaussian broadening of 0.15 eV hwhm.

This figure compares the crystal field multiplet calculation of the $3d^0 \rightarrow 2p^5 3d^1$ transition in Ti^{IV} with the experimental 2p x-ray absorption spectrum of $FeTiO_3$. The titanium ions are surrounded by six oxygen atoms in a (little) distorted octahedron. The value of 10Dq has been set to 1.8 eV. The calculation is able to reproduce all peaks that are experimentally visible. In particular the two small pre-peaks can be nicely observed. The similar spectrum of $SrTiO_3$ has an even sharper spectral shape, related to the perfect octahedral surrounding of Ti^{IV} by oxygen.

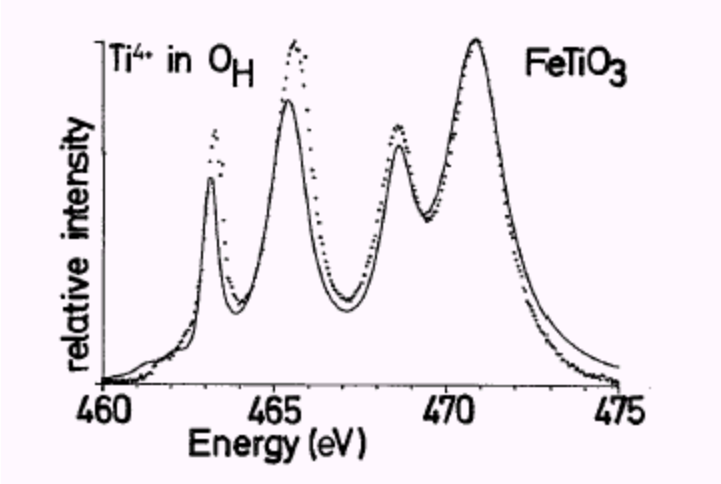

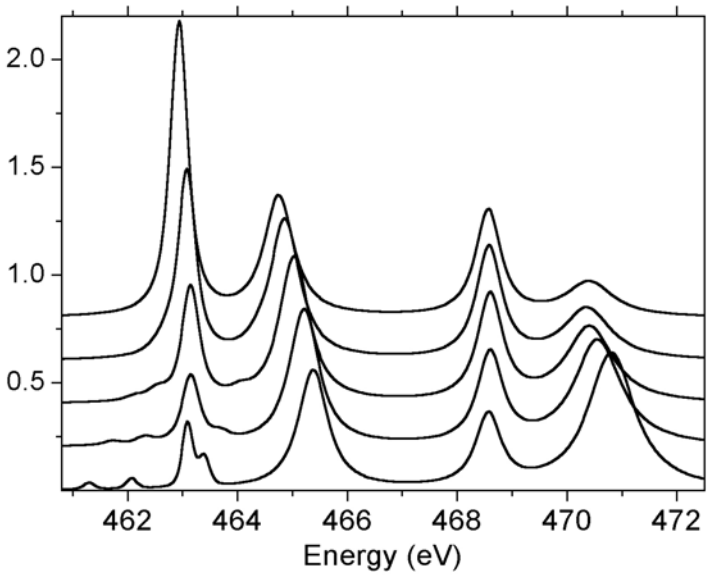

Figure 3.7 The crystal field multiplet calculations for the $3d^0 \rightarrow 2p^5 3d^1$ transition in Ti^{IV}. The atomic Slater-Condon parameters and spin-orbit couplings have been used as given in table 2.14. The bottom spectrum is the crystal field multiplet spectrum with atomic parameters and corresponds to the fifth spectrum in Figure 3.5; i.e. 10Dq is 1.5 eV. Each next spectrum has a value of the Slater integrals further reduced by respectively 25%, 50%, 75% and 99%, i.e. the top spectrum is essentially the single particle (crystal field) result.

Figure 3.7 shows the effect of the pd Slater-Condon parameters on the spectral shape of the $3d^0 \rightarrow 2p^5 3d^1$ transition in Ti^{IV}. The bottom calculation is the same as in Figure 3.5 and used the 80% reduction of the Hartree-Fock values in order to obtain a good estimate of the values in the free atom. In most solids the pd Slater-Condon parameters have essentially the same values as for the free atom, in other words the solid state screening of the pd Slater-Condon parameters is almost zero. The five spectra are calculated by using the same values for the 3d- and 2p-spin-orbit coupling and the same crystal field value of 1.8 eV. The Slater-Condon parameters are rescaled to respectively 80% (bottom), 60%, 40%, 20% and 1% (top). The top spectrum corresponds closely to the single particle picture, where one expects four peaks, respectively the L_3-t_{2g}, the L_3-e_g, the L_2-t_{2g} and the L_2-e_g peak, with respective intensities given by their degeneracies, i.e. 6:4:3:2. This is exactly what is observed in the top spectrum, where it is noted that the intensity ratio is a little obscured by the differences in line width. One can conclude that there is a large difference between the single particle result (top spectrum) and the multiplet result (bottom spectrum). The Slater-Condon parameters have the effect to lower the intensity of the t_{2g} peaks and shift intensity to the e_g peaks. An even larger intensity shift can be observed from the L_3 edge to the L_2 edge and a very clear effect is the creation of additional (pre-)peaks, because additional transitions become allowed.

The files als4ti4c.rcg and ti4ti4c.rac reproduce the calculation for a reduction to 50% of the atomic values. The only parameters that should be changed are the reduction factors in the als4ti4c.rcg file. That is, the second line must be changed from 80998080 to 40994040.

```
    0                       80998080          8065.47800      0000000
    0                       40994040          8065.47800      0000000
```

These numbers are used to multiply the parameters with, before the calculation starts. There are four numbers that are respectively used for the four types of parameters, indicated with a 1, 2, 3 or 4 at the end, i.e.

1. The numbers with a 1 at the end are the 3d3d Slater integrals
2. The numbers with a 2 at the end are the spin-orbit couplings
3. The numbers with a 3 at the end are the 2p3d direct Slater integrals
4. The numbers with a 4 at the end are the 2p3d exchange Slater integrals

Instead of using the reduction factor, one can also change the individual numbers by hand to the required number. One can check in the als4ti4c.org file that the reductions have been performed in the correct manner. The file repeats first the input line and then reports the corrected values. the file gives the *"PARAMETER VALUES IN 8065.5 CM-1",* which identifies with electronvolts and then tells that the values were multiplied with respectively 0.40, 1.00, 0.40 and 0.40, yielding the values for the respective parameters as given below. That is, the blue values are modified to the red values.

```
ECHO:
 TI4+ 2P05 3D01      6  464.8110    3.7762    0.0322    6.3023
4.6284HR9999999
 9
 ECHO:
     2.6334



 TI4+ 2P05 3D01         PARAMETER VALUES IN  8065.5 CM-1 (HR TIMES 0.40
1.00 0.40 0.40)     1  P 5  D 1

                                        EAV            ZETA 1          ZETA
2          F2(12)          G1(12)
          G3(12)

                                     464.811           3.776
0.032           2.521           1.851
           1.053
```

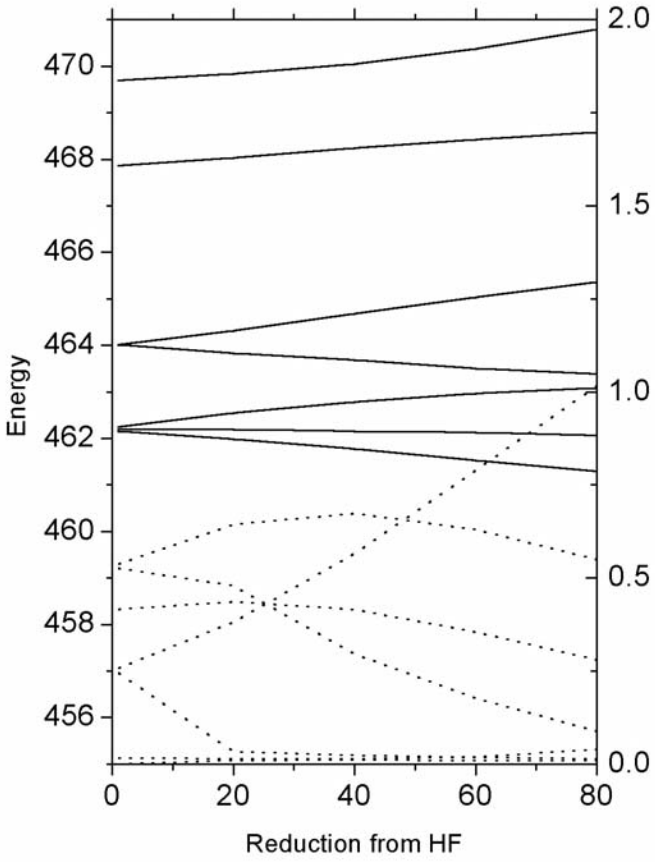

Figure 3.8 The seven peak positions (solid lines, left axis) of Ti^{IV} are given as a function of the Slater-Condon parameters. In addition the intensities (dashed, right axis) are given.

Figure 3.8 shows the shifts in energy and intensity of the seven final states as a function of the Slater-Condon parameters. The solid lines indicate the respective energies (left axis) and one can observe that the four energy levels at the single particle limit on the left split into seven lines if the Slater-Condon parameters are turned on. More precisely, it is only the L_3 edge that is split and its two states are split in five states. The L_2 edge is not split, and in fact because of this the L_2 edge can be expected to stay closer to the single particle result, in particular the energy separation between the t_{2g} and e_g level of the L_2 edge is only little affected. This is important in those cases where the multiplet effects are smaller, such as for the $L_{2,3}$ edges of the 4d-elements. In the case of 4d-elements, their L_2 edge can be expected to be closer related to the single particle picture than the corresponding L_3 edge. The intensity ratio of the seven lines at the single particle limit can be found to be approximately 4:4:3:2:2:0:0. One has to add a 4 and a 2 to 6 to find the single particle result with its 6:4:3:2 ratio.

Chapter 2 CRYSTAL FIELD EFFECTS

Crystal Field Theory

Crystal Field Theory is a well-known model used to explain the electronic properties of transition metal systems. It has been developed in the fifties and sixties against the background of explaining optical spectra and EPR data.

The starting point of the crystal field model is to approximate the transition metal as an isolated atom surrounded by a distribution of charges that should mimic the system, molecule or solid, around the transition metal. At first sight, this seems to be a very simplistic model and one might doubt its usefulness to explain experimental data. However it turned out that such a simple model was extremely successful to explain a large range of experiments, like optical and EPR spectra.

Introduce basic Crystal field model here

Maybe the most important reason of the success of the crystal field model is that the explained properties are strongly determined by symmetry considerations. With its simplicity in concept, the crystal field model could make full use of the results of group theory. Group theory also made possible a close link to atomic multiplet theory. Group theoretically speaking, the only thing crystal field theory does is translate, or branch, the results obtained in atomic symmetry to cubic symmetry and further to any other lower point groups. The mathematical concepts for these branching are well developed.

In this chapter we will focus on these group theoretical results and their effects on the ground states as well as on the spectral shapes. We will first briefly discuss the basics of group theory, to make the unfamiliar reader a little acquainted with the formalism. For any more serious discussion of group theory, the reader is referred to books dedicated to group theory.

A short outline of Group Theory

Group theory is a mathematical framework to deal with symmetry properties of systems. The main result of group theory for x-ray absorption is a systematic method to classify the ground state, final state and transition operator within a certain symmetry. We will concentrate on D_{4h} and O_h symmetry as these two symmetries are most often used for the analysis of x-ray absorption spectra. The discussion of all other point groups follows a similar path.

A group is a set of symmetry elements that satisfy four requirements:

- A group is closed: The product of two elements is also an element of the group.
- Multiplication is associative: The product of three elements e_1, e_2 and e_3 has a result, which is not dependent if the calculation is carried out as $(e_1e_2)e_3$ or $e_1(e_2e_3)$. Note that for most groups $e_1e_2 \neq e_2e_1$. Only for so-called Abelian groups, the multiplication is commutative.
- There is a unit element: A unit element multiplied with any other element yields that element.

- There is an inverse element: for any element of a group there is another element for which the product of the two elements yields the unit element.

The relevant symmetry operations for O_h and D_{4h} symmetry are (a) the identity operation E; (b) rotations, for example 2_z is a two-rotation (180 degrees) around the z-axis; (c) inversion in the centre of symmetry I; (d) reflections σ and (e) rotary reflections S. Rotary reflections are combinations of rotations and reflections into one symmetry operation. In the discussion we will limit ourselves to the identity operation and rotations. The subgroup that can be constructed from rotations and E can be extended by acting on its members by the inversion symmetry I, thereby creating also the (rotary) reflections.

As an example we analyse an object of D_4 symmetry, i.e. the symmetry properties of a square in three-dimensional space. We try to find all symmetry properties that leave the square identical in shape. The square is centred on (0,0) , with the four corners A=(1,1) , B=(-1,1) , C=(-1,-1) and D=(1,-1) , using an x and y -axis. The unit element, indicated with E, leaves the square in place. Another symmetry element is a rotation about the out-of-plane z-axis by 90 degrees, indicated as a fourfold rotation around z, in short 4_z. This symmetry element can be carried out twice to give a rotation of 180 degrees, written as twofold rotation around z or 2_z. Three times 4_z gives a rotation of 270 degrees, which identifies without a rotation of -90 degrees or -4_z. If the symmetry element is carried out four times it yields again the unit element. Table 1 gives the matrices of these four elements. The last column gives the trace, i.e. the sum of the diagonal elements of the symmetry effect written in matrix form. For example, the fourfold rotation around 4_z has a matrix as given in equation 3.1. When one acts with this matrix on corner A one obtains corner B, etc.

$$\begin{pmatrix} 0 & -1 \\ 1 & 0 \end{pmatrix}\begin{pmatrix} 1 \\ 1 \end{pmatrix} = \begin{pmatrix} -1 \\ 1 \end{pmatrix} \qquad (3.1)$$

The last column gives the inverse element. All elements are their own inverse, except 4_z and -4_z which are each others inverse, i.e. $4_z * -4_z = E$. There are more possible symmetry elements. For example a rotation by 180 degrees over the x-axis, 2_x, and similarly a rotation by 180 degrees over the y-axis, 2_y. The last two symmetry operations are rotation by 180 degrees over the diagonal xy-axis 2_{xy} and the x-y-axis 2_{x-y}.

Element	Inverse	ABCD	Trace
E	E	ABCD	2
4_z	-4_z	BCDA	0
2_z	2_z	CDAB	-2
-4_z	4_z	DABC	0
2_x	2_x	BADC	0
2_y	2_y	DCBA	0
2_{xy}	2_{xy}	ADCB	0
2_{x-y}	2_{x-y}	CBAD	0

Table 3.1: The symmetry operations of D_4 symmetry.

Using table 3.1, the four group requirements can be checked. The unit element is E. The inverse of each element is given in the second column. All rotations over 180 degrees are their own inverse. The only two elements that have an inverse different from itself are the rotations by 90 degrees, which are the inverses of each other. The third column gives the change from the four corners ABCD to the positions after the symmetry operation. It can be checked that the group is closed as the product of two elements is always an element of the group. For example 4_z*2_z gives -4_z, etc. The D_4 group is not Abelian, because for example $2_{xy}*2_x$ gives -4_z and 2_x*2_{xy} gives 4_z.

Character Tables

We now shortly outline how to make and use the so-called character table of a group. The first thing to do is to separate the symmetry elements into classes G. Each class includes the same type of symmetry operation. More formally, a class is formed by all elements that are conjugated to each other. B is a conjugate of A if $B = XAX^{-1}$, where X is any element of the group. It can be shown that there are five classes for D_4 symmetry. A one-dimensional class containing E and one containing 2_z. Two-dimensional classes containing 4_z and -4_z , another one with 2_x and 2_y and a third one with 2_{xy} and 2_{x-y}. For example $2_{xy}*2_x*(2_{xy})^{-1}$ gives 2_y, etc. Classes can also be differentiated directly by the nature of their symmetry operations, for example rotations with different angles and rotations over different directions, respectively x, z and xy. The x-axis and y-axis are equivalent hence 2_x and 2_y are member of the same class.

It is now possible to generate the so-called character table. A character table gives for all the possible (irreducible) representations Γ their respective characters χ for each class of symmetry operations. As such a character table is a compact notation of all the symmetry effects of a group and it will be shown below that the character tables are a powerful means to describe the crystal field effect. The character of a symmetry operation for a particular representation is given as the trace of the matrix element. Group theoretical analysis gives the following rules:

1. The number of representations is equal to the number of classes.
2. The total number of symmetry elements h is equal to $\sum_G d_G$, where d_G is the degeneracy or dimension of each class.
3. The dimensions of the representations do obey the fact that $\sum_\Gamma d_\Gamma^2 = h$, where h is the total number of symmetry elements.
4. The characters of the unit element G_1 are given by the dimension of the representation d_Γ.
5. There is a totally symmetric representation Γ_1 that has all its characters equal to 1.
6. The characters of the last representation Γ_5 are given by the traces of the five classes.
7. All classes are orthogonal, i.e. for class i and class j we have $\sum_\Gamma \chi_i \cdot \chi_j = 0$
8. All normalised representations are orthogonal, i.e. for representation i and representation j we have $\sum_G d_G \cdot \chi_i \cdot \chi_j = 0$. The sum of the multiplication of the characters times their dimension equals zero.

Applying these rules to the example of D_4 symmetry, one finds the following: As discussed, D_4 has 5 classes with degeneracies 1, 1, 2, 2 and 2.

1. There are 5 classes that imply 5 representations.
2. There are 8 symmetry elements.
3. The dimensions of the representations must be respectively 1, 1, 1, 1 and 2, i.e. $1^2+1^2+1^2+1^2+2^2=8$.
4. The first column belonging to the class of the unit element G_1 is equal to the respective dimensions of the representations, i.e. 1, 1, 1, 1 and 2.
5. The first representation Γ_1 has characters 1, 1, 1, 1 and 1.
6. The last representation Γ_5 is equal to the traces of the five classes, i.e. 2, -2, 0, 0 and 0.

The boldface part of the character table is filled now.

7. The orthogonality rules allow one to completely fill the character table as given below, for example $\sum_\Gamma \chi_1 \cdot \chi_2 = 0$ implies that $\chi_2=1$ for the representations Γ_2, Γ_3 and Γ_4, etc.

	D_4	(D_{4h})	G_1	G_2	G_3	G_4	G_5
			1	1	2	2	2
Butler	Mulliken	Bethe	E	2_z	4_z, -4_z	2_x, 2_y	2_{xy}, 2_{x-y}
0	A_1	Γ_1	1	1	1	1	1
$\hat{0}$	A_2	Γ_2	1	1	1	-1	-1
2	B_1	Γ_3	1	1	-1	1	-1
$\hat{2}$	B_2	Γ_4	1	1	-1	-1	1
1	E	Γ_5	2	-2	0	0	0

Table 3.2: The character table of D_4 symmetry. Using the rules given above, the character table can be filled.

There are a number of different notations for the five representations. The Bethe notation is most common in physics and the Mulliken notation is most familiar in chemistry. The Butler notation is not often used, but it is included because Butler's computer programmes(Butler 1981) have been included in most multiplet program packages used to calculate spectra.

One can extend the character table of D_4 to D_{4h} by acting on all symmetry elements with the inversion symmetry I. This creates five new classes of (rotary) reflections G_6 to G_{10}. As far as the character table is concerned the effects of I can be condensed to a duplication of the representations into even (gerade) and odd (ungerade) representations, i.e. A_1 is duplicated into A_{1g} and A_{1u}, etc. The characters of G_1 to G_5 are equal for both even and odd representations. In addition for the gerade representations, the characters of G_6 to G_{10} are equal to the characters of G_1 to G_5. In case of the ungerade representations, the characters of G_6 to G_{10} are given by multiplying the characters of G_1 to G_5 by -1. Instead of using the whole 10x10 table of D_{4h} symmetry, it is easier to use the 5x5 table of D_4 and using these rules to find the characters for D_{4h}.

Chapter 2 CRYSTAL FIELD EFFECTS

The character table of octahedral symmetry

The most important crystal field effect in solids is the cubic or octahedral symmetry O_h. We limit ourselves again to rotations and we can use the character rules for O symmetry: O symmetry describes the symmetry of a cube in three dimensions. One can find the following symmetry elements:
(a) Class G_1 is the identity E;
(b) Class G_2 are three-fold rotations around the body diagonals 3_{xyz}. There are 4 body diagonals in a cube, respectively xyz, xy-z, x-yz and -xyz, each containing a 120 degrees and 240 degrees (or -120 degrees) three-fold rotation. In total this yields 8 symmetry elements.
(c) Class G_3 are two-fold rotations around the axes connecting the centres of the faces. There are six faces thus three rotation axes, respectively 2_x, 2_y and 2_z.
(d) Class G_4 are four-fold rotations around the same axes. There are 90 degrees and -90 degrees rotations thus six symmetry elements 4_x, 4_y, 4_z, -4_x, -4_y, -4_z.
(e) Class G_5 are two-fold rotations around the axes connecting the centres of the edges. There are twelve edges thus six symmetry elements 2_{xy}, 2_{x-y}, 2_{xz}, 2_{x-z}, 2_{yz} and 2_{y-z}.
O symmetry has 5 classes with dimensions 1, 8, 3, 6 and 6 hence 24 elements.

1. There are 5 classes that imply 5 representations.
2. There are 24 symmetry elements.
3. The dimensions of the representations are respectively 1, 1, 2, 3 and 3, i.e. $1^2+1^2+2^2+3^2+3^2=24$.
4. The first column belonging to the class of the unit element G_1 is equal to the respective dimensions of the representations, i.e. 1, 1, 2, 3 and 3.
5. The first representation Γ_1 has characters 1, 1, 1, 1 and 1.
6. The last representation Γ_5 is equal to the traces of the five classes, i.e. 3, 0, -1, -1 and 1.

The boldface part of the character table is filled now.

7. The orthogonality rules allow one to fill the character table as given below, for example $\Sigma_\Gamma \chi_1 \cdot \chi_2 = 0$ implies that $\chi_2=1$ for the representations Γ_2, and $\chi_2=-1$ for Γ_3 and $\chi_2=0$ for Γ_4, etc.

The character table of O_h symmetry.							
	O	(O_h)	G_1 1	G_2 8	G_3 3	G_4 6	G_5 6
Butler	Mulliken	Bethe	E	3_{xyz}, 3_{xy-z}, 3_{x-yz}, 3_{-xyz}, -3_{xyz}, -3_{xy-z}, -3_{x-yz}, -3_{-xyz},	2_x, 2_y, 2_z	4_x, 4_y, 4_z, -4_x, -4_y, -4_z	2_{xy}, 2_{x-} 2_{xz}, 2_{x-z} 2_{yz}, 2_{y-z}
0	A_1	Γ_1	1	1	1	1	1
$\hat{0}$	A_2	Γ_2	1	1	1	-1	-1
2	E	Γ_5	2	-1	2	0	0
1	T_1	Γ_3	3	0	-1	1	-1
$\hat{1}$	T_2	Γ_4	3	0	-1	-1	1

The full character table of O_h symmetry can be derived by acting on the symmetry elements with the inversion operator I and applying the rules for the expansion of the 5x5 table to the 10x10 table as given above for D_{4h} symmetry. We will now continue with the description of the crystal field multiplet Hamiltonian, where we will concentrate on O_h and D_{4h} symmetry.

Total Symmetry and Multiplication Tables

The crystal field multiplet calculations for x-ray absorption are performed in total symmetry J, i.e. with the inclusion of the spin-orbit coupling. As discussed in chapter 2, this is necessary because the core hole spin-orbit coupling is large and does not allow to use LS-coupling schemes for the final state of the x-ray absorption process. In spherical symmetry the value of J is given as all values that range from |L-S| to L+S, in steps of 1. If one changes spherical symmetry into cubic symmetry, the orbital momentum L is affected as will be discussed in detail later in this chapter. The spin quantum numbers are in principle not affected, but if one includes the core hole spin-orbit coupling one has to modify the symmetry of the spin quantum number also to cubic symmetry, in order to be able to multiply the L and S symmetry states that are both described with the representations given in table 3.2 and 3.3.

O	A_1	A_2	T_1	T_2	E
A_1	A_1	A_2	T_1	T_2	E
A_2	A_2	A_1	T_2	T_1	E
T_1	T_1	T_2	$T_1 + T_2 + E + A_1$	$T_1 + T_2 + E + A_2$	T_1+T_2
T_2	T_2	T_1	$T_1 + T_2 + E + A_2$	$T_1 + T_2 + E + A_1$	T_1+T_2
E	E	E	T_1+T_2	T_1+T_2	A_1+A_2+E

Table 3.3: The multiplication table of O symmetry.

The multiplication rules that apply in O_h and D_{4h} symmetry can be found directly from their character tables. Table 3.4 gives the multiplication table of O symmetry. For example, multiplying E symmetry with E symmetry yields A_1 plus A_2 plus E symmetry. This can be checked from the character table as follows: $E \otimes E$ gives the characters 4, 1, 4, 0 and 0. The first number gives the dimension. The dimension of 4 implies that the added dimensions of the representations must also be 4. If a T_1 or a T_2 state is one of the representations, one can only add a A_1 or A_2 state. The character tables learn that none of these combinations can yield the characters 4,1,4,0,0. One finds that only the combination $A_1 \oplus A_2 \oplus E$ yields the needed overall characters. In analogy one can determine the complete multiplication table as given in table 3.4. Table 3.5 repeats this procedure for D_4 symmetry.

D4	A_1	A_2	B_1	B_2	E
A_1	A_1	A_2	B_1	B_2	E
A_2	A_2	A_1	B_2	B_1	E
B_1	B_1	B_2	A_1	A_2	E

B_2	B_2	B_1	A_2	A_1	E
E	E	E	E	E	$A_1+A_2+B_1+B_2$

Table 3.4: The multiplication table of D_4 symmetry.

We have now enough group theoretical information to understand the consequences of the crystal field effect on the atomic multiplet states.

The Crystal Field Multiplet Hamiltonian

The crystal field multiplet Hamiltonian consists of the atomic Hamiltonian as outlined in the previous chapter, to which an electrostatic field is added:

$$H_{CF} = H_{ATOM} + H_{FIELD} \tag{3.2}$$

$$H_{ATOM} = \sum_N \frac{p_i^2}{2m} + \sum_N \frac{-Ze^2}{r_i} + \sum_{pairs} \frac{e^2}{r_{ij}} + \sum_N \zeta(r_i)\, l_i \cdot s_i \tag{3.3}$$

$$H_{FIELD} = -e\phi(r) \tag{3.4}$$

The only term added to the atomic Hamiltonian is an electrostatic field, which consists of the electronic charge e times, a potential that describes the surroundings $\phi(r)$. The potential $\phi(r)$ is written as a series expansion of spherical harmonics Y_{LM}'s:

$$\phi(r) = \sum_{L=0}^{\infty} \sum_{M=-L}^{L} r^L A_{LM} Y_{LM}(\psi, \phi) \tag{3.5}$$

The crystal field is regarded as a perturbation to the atomic result. This implies that it is necessary to determine the matrix elements of $\phi(r)$ with respect to the atomic 3d orbitals $<3d|\phi(r)|3d>$. One can separate the matrix elements into a spherical part and a radial part, as was done also for the atomic Hamiltonian in equation 2.6. The radial part of the matrix elements yields the strength of the crystal field interaction. The spherical part of the matrix element can be written completely in Y_{LM} symmetry, where the two 3d-electrons are written as Y_{2m}. This gives:

$$\left\langle Y_{2m_2} \middle| Y_{LM} \middle| Y_{2m_1} \right\rangle = (-1)^{m_2} \sqrt{15(2L+1)/4\pi} \begin{pmatrix} 2 & L & 2 \\ -m_2 & M & m_1 \end{pmatrix} \begin{pmatrix} 2 & L & 2 \\ 0 & 0 & 0 \end{pmatrix} \tag{3.6}$$

The second 3J-symbol is zero unless L is equal to 0, 2 or 4. This limits the crystal field potential for 3d electrons to:

$$\phi(r) = A_{00}Y_{00} + \sum_{M=-2}^{2} r^2 A_{2M} Y_{2M} + \sum_{M=-4}^{4} r^4 A_{4M} Y_{4M} \tag{3.7}$$

The first term $A_{00}Y_{00}$ is a constant. It will only shift the atomic states and it is not necessary to include this term explicitly if one calculates the spectral shape.

Chapter 2 CRYSTAL FIELD EFFECTS

Cubic crystal fields

A large range of systems posses a transition metal ion surrounded by six or eight neighbours. The six neighbours are positioned on the three Cartesian axes, or in other words on the six faces of a cube surrounding the transition metal. They form a so-called octahedral field. The eight neighbours are positioned on the eight corners of the cube and form a so-called cubic field. Both these systems belong to the O_h point group. The character table of O_h symmetry is given above. O_h symmetry is a subgroup of the atomic SO_3 group.

The calculation of the x-ray absorption spectral shape in atomic symmetry involved the calculation of the matrices of the initial state, the final state and the transition. The initial state is given by the matrix element $<3d^N \mid H_{ATOM} \mid 3d^N>$, which for a particular J-value in the initial state gives $\sum_J <J|0|J>$. The same applies for the final state matrix element $<2p^5 3d^{N+1} \mid H_{ATOM} \mid 2p^5 3d^{N+1}>$, where $\sum_{J'} <J'|0|J'>$ is calculated for the values of J' that fulfil the selection rule, i.e. J'=J-1, J and J+1. The dipole matrix element $<3d^N \mid p \mid 2p^5 3d^{N+1}>$ implies the calculation of all matrices that couple J and J': $\sum_{J,J'} <J|1|J'>$. To calculate the x-ray absorption spectrum in a cubic crystal field, these atomic transition matrix elements must be branched to cubic symmetry. This is essentially the only task to fulfil.

SO_3		O_h (Butler)	O_h (Mulliken)
S	0	0	A_1
P	1	1	T_1
D	2	$2 + \hat{1}$	$E+T_2$
F	3	$\hat{0} + 1 + \hat{1}$	$A_2+T_1+T_2$
G	4	$0 + 1 + 2 + \hat{1}$	$A_1+E+T_1+T_2$

Table 3.5 Branching rules for the symmetry elements by going from SO_3 symmetry to O_h symmetry.

Table 3.6 gives the branching from SO_3 to O_h symmetry. This table can be determined from group theory(Butler 1981). This table implies that an S symmetry state in atomic symmetry branches only to a A_1 symmetry state in octahedral symmetry. This is the case, because the symmetry elements of an s-orbital in O_h symmetry are determined by the character table of A_1 symmetry, i.e. whatever symmetry operation one applies an s-orbital remains an s-orbital. This is not the case for the other orbitals. For example, a p-orbital can be described with the characters of the T_1 symmetry state in O_h symmetry, for example the class G_3, a two-fold rotation around x, inverts the p-orbital. A d-orbital or a D symmetry state in SO_3, branches to E plus T_2 symmetry states in octahedral symmetry. This can be related to the character table by adding the characters of E and T_2 symmetry, yielding the overall characters 5, -1, 1, -1 and 1, which describe the properties of d-orbitals in O_h symmetry, i.e. the dimension of a d-orbital is 5 and the class G_4 (a fourfold rotation around x) inverts the d-orbitals. This is a well-known result: A 3d electron is separated into t_{2g} and e_g electrons in octahedral symmetry, where the symmetries include the gerade-notation of the complete O_h character table.

One can make the following observations: The dipole transition operator has p-symmetry and is branched to T_1 symmetry. Having a single symmetry in O_h symmetry, there will be no dipolar angular dependence in x-ray absorption. The quadrupole transition operator has d-symmetry and is split into two operators in O_h symmetry, in other words there will be different quadrupole transitions in different directions. The Hamiltonian is given by the unity representation A_1 of the symmetry under consideration. In O_h symmetry the atomic G-symmetry state branches into the A_1 Hamiltonian, which is a confirmation of equation 3.7 as given above.

We can lower the symmetry from octahedral O_h to tetragonal D_{4h} and describe this symmetry lowering again with a branching table. Table 3.4 gives the branching table from O_h to D_{4h} symmetry.

O_h (Butler)	O_h (Mulliken)	D_{4h} (Butler)	D_{4h} (Mulliken)
0	A_1	0	A_1
$\hat{0}$	A_2	2	B_1
1	T_1	$1 + \hat{0}$	$E + A_2$
$\hat{1}$	T_2	$1 + \hat{2}$	$E + B_2$
2	E	0 + 2	$A_1 + B_1$

Table 3.6 Branching rules for the symmetry elements by going from O_h symmetry to D_{4h} symmetry.

An atomic s-orbital is branched to D_{4h} symmetry according to the branching series $S \rightarrow A_1 \rightarrow A_1$. In other words it is still the unity element, and it will always be the unity element in all symmetries. An atomic p-orbital is branched according to $P \rightarrow T_1 \rightarrow E+A_2$. Adding the characters of E and A_2 yields 3, -1, 1, -1 and -1, implying that a two-fold rotation around the z-axis inverts a p-orbital, etc. Similarly an atomic d-orbital is branched according to $D \rightarrow E+T_2 \rightarrow A_1+B_1+E+B_2$. Adding the characters of these four representations yields 5, 1, -1, 1 and 1. The dipole transition operator has p-symmetry and hence is branched to $E+A_2$ symmetry, in other words the dipole operator is described with two operators in two different directions implying an angular dependence in the x-ray absorption intensity. The quadrupole transition operator has d-symmetry and is split into four operators in D_{4h} symmetry, in other words there will be four different quadrupole transitions in different directions/symmetries. The Hamiltonian is given by the unity representation A_1. Similarly as in O_h symmetry, the atomic G-symmetry state branches into the Hamiltonian in D_{4h} symmetry according to the series $G \rightarrow A_1 \rightarrow A_1$. In addition it can be seen that the E symmetry state of O_h symmetry branches to the A_1symmetry state in D_{4h} symmetry. The E symmetry state in O_h symmetry is found from the D and G atomic states. This implies that also the series $G \rightarrow E \rightarrow A_1$ and $D \rightarrow E \rightarrow A_1$ become part of the Hamiltonian in D_{4h} symmetry. This is again a confirmation of equation 3.6, where we find that the second term $A_{2M}Y_{2M}$ is part of the Hamiltonian in D_{4h} symmetry. The three branching series in D_{4h} symmetry are in Butlers notation (Butler 1981)given as $4 \rightarrow 0 \rightarrow 0$, $4 \rightarrow 2 \rightarrow 0$ and $2 \rightarrow 2 \rightarrow 0$ and the radial parameters related to these branches are indicated as X_{400}, X_{420}, and X_{220}. The X_{400} term is important already in O_h symmetry. This term is closely related to the cubic crystal field term 10Dq as will be discussed below.

Chapter 2 CRYSTAL FIELD EFFECTS

The definitions of the Crystal Field parameters

In order to compare the X_{400}, X_{420}, and X_{220} definition of crystal field operators to other definitions like Dq, Ds, Dt, we compare their effects on the set of 3d-functions. The most straightforward way to specify the strength of the crystal field parameters is to calculate the energy separations of the 3d-functions. In O_h symmetry there is only one crystal field parameter X_{40}. This parameter is normalised in a manner that creates unitary transformations in the calculations. The result is that it is equal to $1/18*\sqrt{30}$ times 10Dq, or 0.304 times10Dq.

In tetragonal symmetry (D_{4h}) the crystal field is given by three parameters, X_{400}, X_{420} and X_{220}. An equivalent description is to use the parameters Dq, Ds and Dt. Table 3.8 gives the action of the X_{400}, X_{420} and X_{220} on the 3d-orbitals and relates the respective symmetries to the linear combination of X parameters, the linear combination of the Dq, Ds and Dt parameters and the specific 3d-orbital(s) of that particular symmetry.

Γ	Energy expressed in X-terms	Energy in D-terms	orbitals
b_1	$30^{-½}\cdot X_{400} - 42^{-½}\cdot X_{420} - 2\cdot 70^{-½}\cdot X_{220}$	6Dq+2Ds–1Dt	$3d_{x2-y2}$
a_1	$30^{-½}\cdot X_{400} + 42^{-½}\cdot X_{420} + 2\cdot 70^{-½}\cdot X_{220}$	6Dq–2Ds–6Dt	$3d_{z2}$
b_2	$-2/3\cdot 30^{-½}\cdot X_{400} + 4/3\cdot 42^{-½}\cdot X_{420} - 2\cdot 70^{-½}\cdot X_{220}$	-4Dq+2Ds–1Dt	$3d_{xy}$
e	$-2/3\cdot 30^{-½}\cdot X_{400} - 2/3\cdot 42^{-½}\cdot X_{420} + 70^{-½}\cdot X_{220}$	-4Dq-1Ds+4Dt	$3d_{xz}$, $3d_{yz}$

Table 3.7 The energy of the 3d orbitals is expressed in X_{400}, X_{420} and X_{220} in the second column and in Dq, Ds and Dt in the third column.

From this table we can relate both notations and write X_{400}, etc as a function of Dq, Ds and Dt.

- $X_{400} = 6\cdot 30^{½}\cdot Dq - 7/2\cdot 30^{½}\cdot Dt$
- $X_{420} = -5/2\cdot 42^{½}\cdot Dt$
- $X_{220} = -70^{½}\cdot Ds$.

The inverse relationship imply:

- $Dq = 1/6\cdot 30^{-½}\cdot X_{400} - 7/30\cdot 42^{-½}\cdot X_{420}$
- $Ds = -70^{-½}\cdot X_{220}$
- $Dt = -2/5\cdot 42^{-½}\cdot X_{420}$

These relations allow the quick transfer from for example the values of Dq, Ds and Dt from optical spectroscopy to the X-values as used in x-ray absorption.

$3d^0$ systems in lower symmetries

If one reduces the symmetry further from O_h to D_{4h} the seven lines in the x-ray absorption spectrum of Ti^{IV} split further. The respective degeneracies of the representations in O^h symmetry and the corresponding symmetries in D_{4h} symmetry are collected in this table.

Γ in O_h	Deg.		Γ in D_{4h}		Deg.
A_1	2	A_1	A_1	2+5	7
A_2	3	B_1	A_2	7	7
T_1	7	$E+A_2$	B_1	3+5	8
T_2	8	$E+B_2$	B_2	8	8
E	5	A_1+B_1	E	7+8	15
$\sum$	25				45

A $2p^5 3d^1$ configuration has twelve representations in SO_3 symmetry that are branched to 25 representations in a cubic field. These 25 representations are further branched to 45 representations in D_{4h} symmetry, of the overall degeneracy of 60. From these 45 representations, 22 are of interest for the calculation of the x-ray absorption spectral shape, because they have either E or A_2 symmetry. There are now two different final state symmetries possible because the dipole operator is split into two representations. The spectrum of two-dimensional E-symmetry relates to the in-plane direction of the tetragonal structure, while the one-dimensional A_2-symmetry relates to the out-of-plane direction.

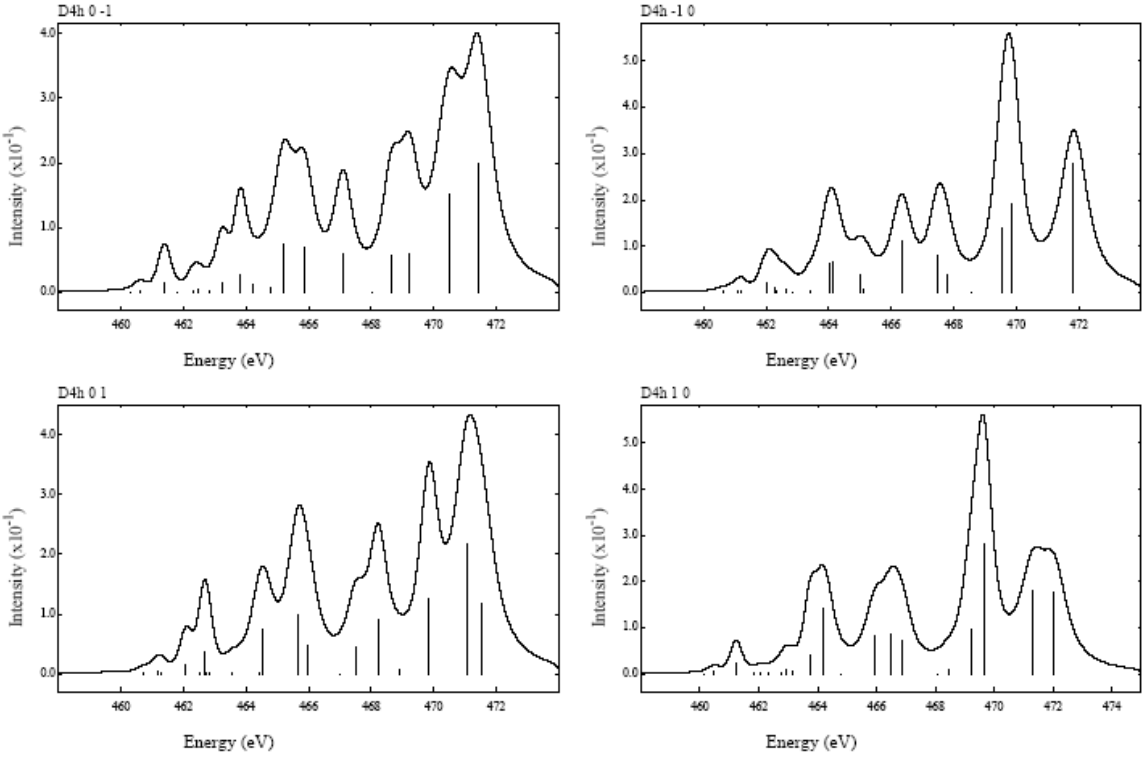

This figure shows the crystal field multiplet calculation of Ti^{IV} in D_{4h} symmetry, using the files als4ti4d4h.rcg and als4ti4d4h.rac. Four calculations have been performed. The value of the X40 branch was set to 7.0 in all cases and for the two other parameters X42 and X22 the combinations (5,0), (-5,0), (0,5) and (0,-5) were made. The four outputfiles have been saved as als4ti4d4hm0.ora, etc. The figure is made with the file als4ti4d4h.plo. One can use the expressions on the previous page to calculate the values of 10Dq, Ds and Dt and the energy positions of the different 3d-orbitals. For example, the parameters (X40,X42,x22)= (7,0,5) relate to (10Dq, Dt,Ds) = (2.13, 0, 0.597), etc.

Lower symmetry and angular dependence

Examples of this angular dependence in D_{4h} and lower symmetries can be found in the study of interfaces, surfaces and adsorbates. A detailed study of the symmetry effects on the calcium 2p x-ray absorption spectra at the surface and in the bulk of CaF_2 did clearly show the ability of the multiplet calculations to reproduce the spectral shapes both in the bulk as at the reduced C_{3v} symmetry of the surface (see himpsel91a.pdf).

The group of Anders Nillson performed potassium 2p x-ray absorption experiments of potassium adsorbed on Ni(100) as well as the co-adsorption system CO/K/Ni(100) hasselstrom00a.pdf. The figure on the right shows the K 2p x-ray absorption spectra of K/Ni(100) compared with CO/K/Ni(100). Note that potassium can be considered as K+, which is a 3d0 system similar to Ti4+. The co-adsorption system shows significantly more structural details, which is caused by the strong (crystal) field of the CO molecules on the K ions. The CO and K adsorbates can be considered to be placed on respectively the black and white squares of a checkers game. Each K ion is surrounded by the four CO molecules in plane as well as the nickel surface below and vacuum above. This C_{4v} symmetry field is expected to have significant angular dependence between the x-ray absorption spectral shape in plane and out-of-plane. This is shown in the bottom half of the figure. Two asymmetric peaks are visible for (near) grazing incidence and four peaks are visible at normal incidence.

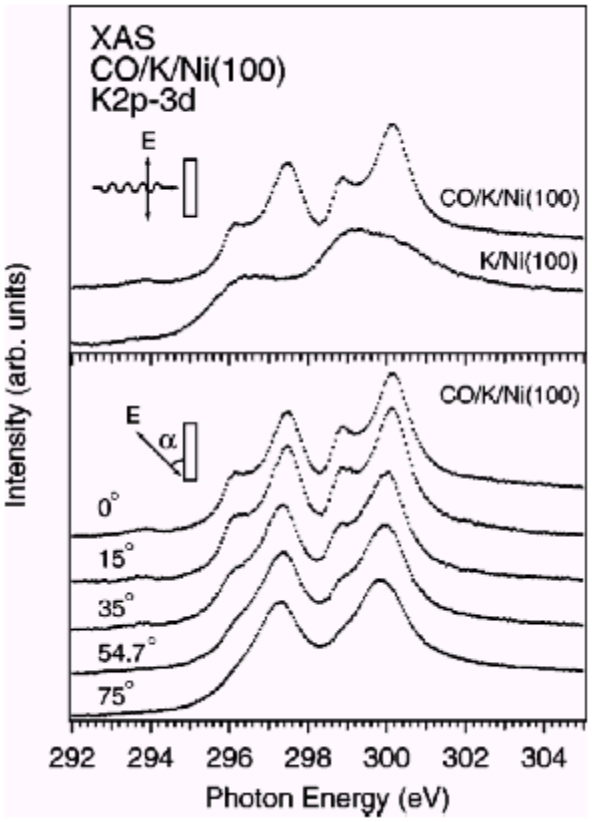

This figure shows a crystal field multiplet calculation of the K 2p x-ray absorption spectrum in C_{4v} symmetry. The calculation reproduces the two asymmetric peaks that are visible for grazing incidence and four peaks at normal incidence. At normal incidence the electric field of the x-ray probes the bonds that are in the direction along the Ni(100) surface. These are the bonds/interactions between the K ion and the CO molecules. Because of the four CO molecules surrounding the K ion, this interaction induced a clear energy difference between the $3d_{x2-y2}$ orbitals pointing towards the CO molecules and $3d_{xy}$ orbitals pointing in between the CO molecules. It is the energy difference between these orbitals that causes the two peaks to be present. This effect can be nicely shown by using exactly the same crystal field parameters and reducing the Slater-Condon parameters to zero. This single particle limit is shown in the bottom half of the figure.

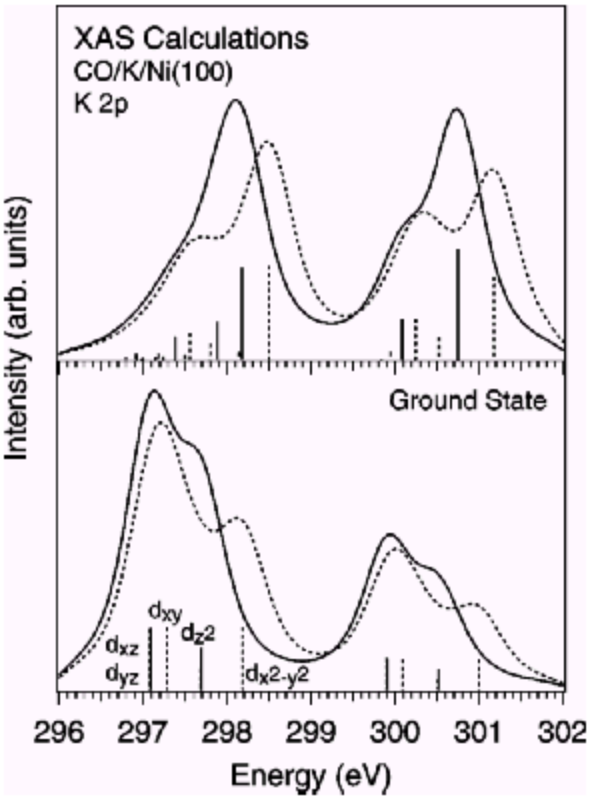

Crystal field effects on 3dN systems

The energies of the 3dN configurations

Table 2.6 gives the energy levels of a $3d^8$ configuration and table 2.15 gives the ground states of the $3d^N$ configurations in atomic symmetry. The crystal field effect modifies these energy levels by the additional terms in the Hamiltonian as given in equation 3.6. We will use the $3d^8$ configuration as an example to show the effects of the O_h and D_{4h} symmetry. Assuming for the moment that the 3d spin-orbit coupling is zero, in O_h symmetry the five term symbols in spherical symmetry split into eleven term symbols. Their respective energies can be calculated by adding the effect of the cubic crystal field 10Dq to the atomic energies. The diagrams of the respective energies with respect to the cubic crystal field (normalised to the Racah parameter B) are known as the Tanabe-Sugano diagrams.

	Relative Energy	Symmetries in O_h	Symmetries in D_{4h}
^1S	4.6 eV	$^1A_1$	$^1A_1$
^3P	0.2 eV	$^3T_1$	$^3E+^3A_2$
^1D	-0.1 eV	$^1E + ^1T_2$	$^1A_1+^1B_1 + ^1E+^1B_2$
^3F	-1.8 eV	$^3A_2 + ^3T_1 + ^3T_2$	$^3B_1 + ^3E + ^3A_2 + ^3E + ^3B_2$
^1G	0.8 eV	$^1A_1+^1T_1+^1T_2+^1E$	$^1A_1+^1E + ^1A_2+^1E+^1B_2+^1A_1+^1B_1$

Table 3.8 The five symmetry states of a $3d^8$ configuration in SO_3 symmetry and their respective energies for Ni^{II} are given in columns 1 and 2. Column 3 gives the respective symmetries of these states in O_h symmetry and column 4 in D_{4h} symmetry. In both cases the spin-orbit coupling has not yet been included.

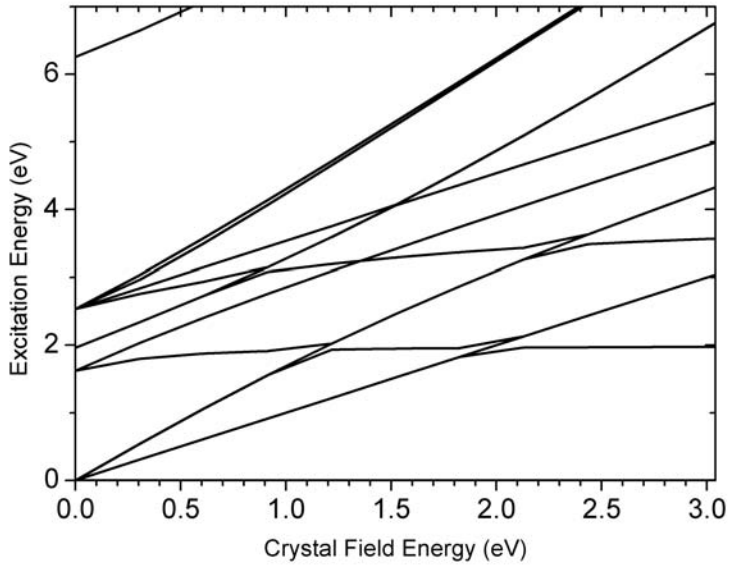

This figure gives the Tanabe-Sugano diagram for the $3d^8$ configuration. The ground state of a $3d^8$ configuration in O_h symmetry has $^3A_2$ symmetry. It is set to zero in figure 3.1. If the crystal field energy is 0.0 eV one has effectively the atomic multiplet states. From low energy to high energy, one can observe respectively the ^3F, ^1D, ^3P, ^1G and ^1S states. Including a finite crystal field strength splits these states, for example the ^3F state is split into $^3A_2$ + $^3T_1$ + $^3T_2$ as indicated in table 3.9. At higher crystal field strengths states start to change their order and they cross. If states actually cross each other or show non-crossing behaviour depends on the fact if their symmetries allow them to form a linear combination of states. This also depends on the inclusion of the 3d spin-orbit coupling.

Generating Tanabe-Sugano diagrams from the multiplet calculations

The crystal field multiplet calculations use a single configuration as their ground state, in other words its ground state can be found from the Tanabe Sugano diagram. This also implies that the energies of the TSD are calculated in the crystal field multiplet calculation. The numbers are given in the ora files. If we use the files als5ni2.rcg and als5ni2.rac (which are identical to the als1ni2 files), we find in the als5ni2.ora file the following lines:

```
 H   H  AAA  M   M IIIII L     TTTTT  OOO  N   N IIIII  AAA  N   N
 H   H A   A MM MM   I   L       T   O   O NN  N   I   A   A NN  N
 HHHHH AAAAA M M M   I   L       T   O   O N N N   I   AAAAA N N N
 H   H A   A M   M   I   L       T   O   O N  NN   I   A   A N  NN
 H   H A   A M   M IIIII LLLLL   T    OOO  N   N IIIII A   A N   N

 CALCULATIONS for ACTOR:HAMILTONIAN     GROUND

       CALCULATING MATRIX for TRIAD  1  (  0+   0+   0+ 0)  (4*4)
       MATRIX HAS 4 ZERO, 12 REAL and 0 COMPLEX ELEMENTS

       DIAGONALIZATION


       ---- EIGENVALUES ----

                  1         2         3         4
   KET/PURE    3 0.92    4 0.93    1 0.92    2 0.94
     EIGVAL -0.801748  0.603819  0.943165  5.315486



       CALCULATING MATRIX for TRIAD  6  (  1+   0+   1+ 0)  (4*4)
```

```
     MATRIX HAS 4 ZERO, 12 REAL and 0 COMPLEX ELEMENTS

     DIAGONALIZATION

     ---- EIGENVALUES ----

               1         2         3         4
KET/PURE    2 0.52    3 0.47    1 0.91    4 0.99
  EIGVAL -1.472040 -0.734825  0.914685  1.097910

     CALCULATING MATRIX for TRIAD 21  (  2+   0+   2+ 0)  (5*5)
     MATRIX HAS 6 ZERO, 19 REAL and 0 COMPLEX ELEMENTS

     DIAGONALIZATION

     ---- EIGENVALUES ----

               1         2         3         4         5
KET/PURE    4 0.76    3 0.40    1 0.41    2 0.90    5 0.74
  EIGVAL -1.492799 -0.730041 -0.515086  0.855732  1.906725

     CALCULATING MATRIX for TRIAD 31  ( ^1+   0+  ^1+ 0)  (6*6)
     MATRIX HAS 10 ZERO, 26 REAL and 0 COMPLEX ELEMENTS

     DIAGONALIZATION

     ---- EIGENVALUES ----

               1         2         3         4         5         6
KET/PURE    5 0.52    1 0.47    4 0.53    3 0.79    2 0.83    6 0.84
  EIGVAL -2.572434 -1.420765 -0.629293  0.391811  0.886141  1.968931

     CALCULATING MATRIX for TRIAD 46  ( ^0+   0+  ^0+ 0)  (1*1)
     MATRIX HAS 0 ZERO, 1 REAL and 0 COMPLEX ELEMENTS

     DIAGONALIZATION

     ---- EIGENVALUES ----

               1
KET/PURE    1 1.00
  EIGVAL -1.400139
```

The numbers in bold red are the respective energies from the TSD. Collecting the energies yields:

```
A1 -0.801748 0.603819  0.943165  5.315486
T1 -1.472040 -0.734825  0.914685  1.097910
E  -1.492799 -0.730041 -0.515086  0.855732  1.906725
T2 -2.572434 -1.420765 -0.629293  0.391811  0.886141  1.968931
A2 -1.400139
```

The energies and symmetries are given in total symmetry. The ground state is found at -2.572434 eV and has T2 symmetry. This is the 3A2 ground state of a 3d8 configuration, which in total symmetry gives A2xT1=T2 symmetry. The next lowest states are a number of states around –1.45 eV. In total there are four of these states with the symmetries T1, E, T2 and A2. Adding the degeneracies yields a 3+2+3+1= 9-fold degenerate state. This is the 3T2 state, which can be checked by multiplying T1 with T2, yielding the 4 symmetries as given. Below the lowest 5 states have been identified. Continuing in this way yields the complete TSD.

```
A1                    -0.801748                    0.603819  0.943165  5.315486
T1           -1.472040 -0.734825                    0.914685  1.097910
E            -1.492799 -0.730041 -0.515086          0.855732  1.906725
T2 -2.572434 -1.420765 -0.629293           0.391811  0.886141  1.968931
A2           -1.400139
```

3A2 3T2 3T1 1E 1T2

The determination of the TSD symmetries using the method as given above becomes rather complex if the ground state has many states, say between 3d3 and 3d7. Things become significantly simpler if one switches the ground state 3d spin-orbit coupling off. In doing so, the states of a certain symmetry state become exactly degenerate.

The files als5ni2z.rcg and als5ni2z.rac use a zero 3d spin-orbit coupling. The only change that must be made is changed the value 0.0832 in the ground state to 0.0002. (check that this is done by inspecting the file als5ni2z.rcg).

```
Ni2+ 2p06 3d08     4    0.0000   12.2341    7.5981    0.0832    0.0000HR99999999
Ni2+ 2p06 3d08     4    0.0000   12.2341    7.5981    0.0002    0.0000HR99999999
```

This yields an als5ni2z.ora file that has the TSD without the inclusion of the 3d spin-orbit coupling.

```
A1                    -0.687617           0.599870  0.883427           5.306541
T1           -1.441638 -0.687618                    0.883427  1.093059
E            -1.441639 -0.687617 -0.630865          0.883427  1.901225
T2 -2.558384 -1.441639 -0.687618           0.422527  0.883427           1.964579
A2           -1.441639
```

3A2 3T2 3T1 1E 1A1 1T2 3T1 1T1 1E 1A1 1T2

The symmetries one finds are exactly those as determined from group theory arguments above. Note that the ground state is a pure T2 symmetry state in double

group symmetry. This implies that it cannot be split and as such is not affected by the 3d spin-orbit coupling.

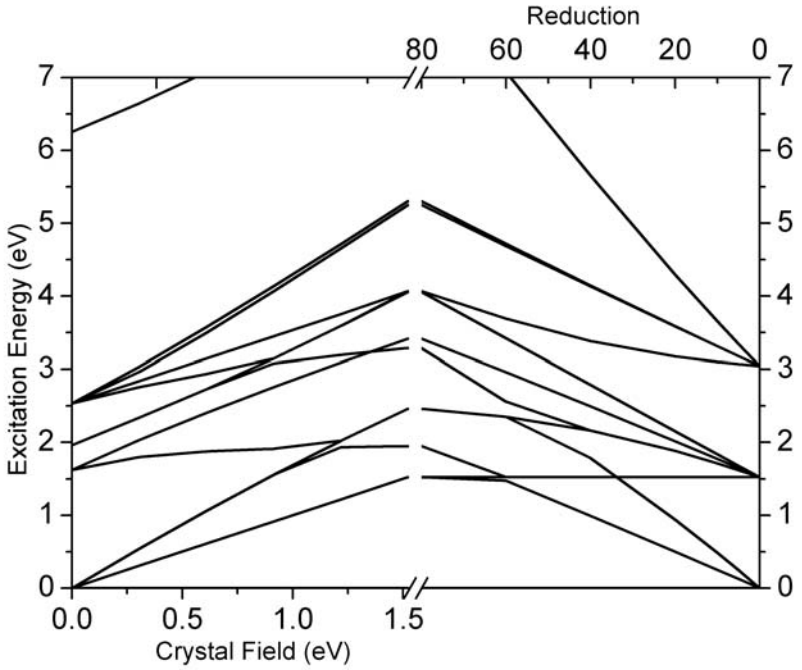

The figure shows the effect of the reduction of the Slater-Condon parameters. The figure is the same as figure 3.1 up to a crystal field of 1.5 eV. Then for this crystal field value the Slater-Condon parameters have been reduced from their atomic value, indicated with 80% of their Hartree-Fock value to 0%. The spectrum for 0% has all its Slater-Condon parameters reduced to zero, In other words the 2p3d coupling has been turned of and one essentially observes the energies of a $3d^8$ configuration, i.e. of a two 3d-holes. This single particle limit has three configurations, respectively the two holes in $e_g e_g$, $e_g t_{2g}$ and $t_{2g} t_{2g}$ states. The energy difference between $e_g e_g$ and $e_g t_{2g}$ is exactly the crystal field value of 1.5 eV. This figure shows nicely the transition from the single particle picture to the multiplet picture for the $3d^8$ ground state.

With the files als5ni2b.rcg and als5ni2b.rac we can reproduce the case that the 3d3d Slater-integrals are switched off. One obtains the following result for the eigenvalues in the initial state:

```
A1 -1.340094 -0.223349                      0.893396  0.893396
T1           -0.223349 -0.223349 -0.223349  0.893396
E  -1.340094 -0.223349 -0.223349            0.893396  0.893396
T2 -1.340095 -0.223349 -0.223349 -0.223349  0.893396  0.893396
A2           -0.223349
```

ee et tt

The lowest energy state has two holes in the eg level. Its dimension is 1+2+3=6. The next level has a hole in eg and a hole in t2g. Its dimension is 1+9+4+9+1=24. The highest energy state has two holes in the t2g level with dimension 2+3+4+6=15. These degeneracies can be determined from the calculation of the possible number of

ways one can put two holes in an eg level. There are 4 eg orbitals, implying that the first hole has 4 possibilities, the second 3 and their product must be divided by 2, giving 4*3/2 = 6. Similarly for two t2g holes this gives 6*5/2=15. For a hole in eg plus a hole in t2g the number of possibilities is 6*4=24.

The intermediate states on the right side of figure 3.2 can be determined using the files als5ni2z.rcg and als5ni2z.rac, by setting the first reduction factor from 80 to, for example, 60, 40 and 20, i.e. the following line in als5ni2z.rcg is changed.

```
0                80998080          8065.47800      0000000
0                40998080          8065.47800      0000000
```

One can make the grid of the TSD as fine as one likes by calculating a large number of states. Interesting things happen if one is close to a crossing point, for example a high-spin to low-spin transition. If the 3d spin-orbit coupling is set to zero high-spin and low-spin states just cross as they are not coupled. However, if the 3d spin-orbit coupling is switched on, the ground state could become a mixture of high-spin and low-spin. An example can be found in piamonteze05a.pdf.

X-ray absorption calculations of 3dN systems

The results of Ti4+ and Ni2+ can be generalised to all 3d transition metal ions.

General calculation $3d^N \rightarrow 2p^5 3d^{N+1}$ in SO_3 symmetry		
Initial State	Transition	Final State
<0 | 0 | 0>	<0 | 1 | 1>	<0 | 0 | 0>
<1 | 0 | 1>	<1 | 1 | 0> <1 | 1 | 1> <1 | 1 | 2>	<1 | 0 | 1>
<2 | 0 | 2>	<2 | 1 | 1> <2 | 1 | 3>	<2 | 0 | 2>
<3 | 0 | 3>	<3 | 1 | 2> <3 | 1 | 3> <3 | 1 | 4>	<3 | 0 | 3>
<4 | 0 | 4>	<4 | 1 | 3> <4 | 1 | 4>	<4 | 0 | 4>

Table 3.9 The matrix elements in SO_3 symmetry needed for the calculation of 2p x-ray absorption. Boldface matrix elements apply to a $3d^0$ configuration.

Table 3.14 gives all matrix element calculations that are possible for $3d^N \rightarrow 2p^5 3d^{N+1}$ transitions in SO_3 symmetry for J-values up to 4.

We will use the transitions $3d^0 \rightarrow 2p^5 3d^1$ and $3d^8 \rightarrow 2p^5 3d^9$ as examples. $3d^0$ has a 1S0 ground state with only a J=0 symmetry state. This limits the calculation for the ground state spectrum to only one ground state, one transition and one final state matrix element, i.e. <0 | 1 | 1>. 3d8 has a 3F4 ground state. This implies that there are two different matrix elements that have to be calculated <4 | 1 | 3> and <4 | 1 | 4>, as we have seen in chapter 3.

We are now going to apply the SO3→Oh branching rules to these tables.

General calculation $3d^N \rightarrow 2p^5 3d^{N+1}$ in O_h symmetry		
Initial State	Transition	Final State
$<A_1 \mid A_1 \mid A_1>$	$<A_1 \mid T_1 \mid T_1>$	$<A_1 \mid A_1 \mid A_1>$
$<T_1 \mid A_1 \mid T_1>$	$<T_1 \mid T_1 \mid A_1>$ $<T_1 \mid T_1 \mid T_1>$ $<T_1 \mid T_1 \mid E>$ $<T_1 \mid T_1 \mid T_2>$	$<T_1 \mid A_1 \mid T_1>$
$<E \mid A_1 \mid E>$	$<E \mid T_1 \mid T_1>$ $<E \mid T_1 \mid T_2>$	$<E \mid A_1 \mid E>$
$<T_2 \mid A_1 \mid T_2>$	$<T_2 \mid T_1 \mid T_1>$ $<T_2 \mid T_1 \mid E>$ $<T_2 \mid T_1 \mid T_2>$ $<T_2 \mid T_1 \mid A_2>$	$<T_2 \mid A_1 \mid T_2>$
$<A_2 \mid A_1 \mid A_2>$	$<A_2 \mid T_1 \mid T_2>$	$<A_2 \mid A_1 \mid A_2>$

Table 3.10 The matrix elements in O_h symmetry needed for the calculation of 2p x-ray absorption. Boldface matrix elements apply to a $3d^0$ configuration.

In octahedral symmetry one has to calculate five matrices for the initial and final states and thirteen transition matrices. Note that this is a general result for all even numbers of 3d electrons, as there are only these five symmetries in O_h symmetry. The case of an odd number of electrons will be described below. In the 3d0 case, the ground state branches to 1A1, with total symmetry A1xA1=A1. This again limits the calculation to only one transition matrix <A1|T1|T1>. We have seen this in the ora outputfiles that contain the seven lines of the <A1|T1|T1> transition at the end. In the 3d8 case the ground state is 3A2, which in total symmetry yields a T2 ground state. Using the table above, this implies that four dipole matrix elements must be calculated for the ground state $<T_2 \mid T_1 \mid T_1>$, $<T_2 \mid T_1 \mid E>$, $<T_2 \mid T_1 \mid T_2>$ and $<T_2 \mid T_1 \mid A_2>$.

These rules can also be found in the als5ni2.ora outputfiles. If we look at the file the program describes all triads that are calculated:

```
CALCULATIONS for ACTOR:PLANE           TRANSI

       CALCULATING MATRIX for TRIAD  5  (  0+   1-   1- 0)  (4*7)
       MATRIX HAS 21 ZERO, 7 REAL and 0 COMPLEX ELEMENTS

       CALCULATING MATRIX for TRIAD 17  (  1+   1-   0- 0)  (4*2)
       MATRIX HAS 5 ZERO, 3 REAL and 0 COMPLEX ELEMENTS

       CALCULATING MATRIX for TRIAD 18  (  1+   1-   1- 0)  (4*7)
       MATRIX HAS 19 ZERO, 9 REAL and 0 COMPLEX ELEMENTS

       CALCULATING MATRIX for TRIAD 19  (  1+   1-   2- 0)  (4*5)
       MATRIX HAS 14 ZERO, 6 REAL and 0 COMPLEX ELEMENTS

       CALCULATING MATRIX for TRIAD 20  (  1+   1-  ^1- 0)  (4*8)
       MATRIX HAS 21 ZERO, 11 REAL and 0 COMPLEX ELEMENTS
```

```
      CALCULATING MATRIX for TRIAD 29  (  2+   1-   1- 0)  (5*7)
      MATRIX HAS 23 ZERO, 12 REAL and 0 COMPLEX ELEMENTS

      CALCULATING MATRIX for TRIAD 30  (  2+   1-  ^1- 0)  (5*8)
      MATRIX HAS 27 ZERO, 13 REAL and 0 COMPLEX ELEMENTS

      CALCULATING MATRIX for TRIAD 42  ( ^1+   1-   1- 0)  (6*7)
      MATRIX HAS 27 ZERO, 15 REAL and 0 COMPLEX ELEMENTS

      CALCULATING MATRIX for TRIAD 43  ( ^1+   1-   2- 0)  (6*5)
      MATRIX HAS 21 ZERO, 9 REAL and 0 COMPLEX ELEMENTS

      CALCULATING MATRIX for TRIAD 44  ( ^1+   1-  ^1- 0)  (6*8)
      MATRIX HAS 30 ZERO, 18 REAL and 0 COMPLEX ELEMENTS

      CALCULATING MATRIX for TRIAD 45  ( ^1+   1-  ^0- 0)  (6*3)
      MATRIX HAS 9 ZERO, 9 REAL and 0 COMPLEX ELEMENTS

      CALCULATING MATRIX for TRIAD 50  ( ^0+   1-  ^1- 0)  (1*8)
      MATRIX HAS 3 ZERO, 5 REAL and 0 COMPLEX ELEMENTS
```

One finds that triads 42, 43, 44 and 45 have a T2 (^1+) initial state. These are the important matrices for Ni2+ calculations.

Later in the als5ni2.ora the transformed matrices are given for these four triads. For example for triad 42, the file yields:

```
TRANSFORMED MATRIX for TRIAD 42  ( ^1+   1-   1- 0) (6*7)  DIM :3:3:3   ACTOR
PLANE

      ---- MATRIX ----      PRINTTRANS

 BRA/KET :   852.903   854.301   855.088   855.312   856.419   871.640   873.099
-------------------------------------------------------------------------------
 -2.57243:  0.084753  0.000524  0.073496  0.054465  0.000005  0.139178  0.005166
 -1.42076:  0.010636  0.028672  0.181098  0.000208  0.040343  0.069081  0.074203
 -0.62929:  0.013535  0.044253  0.100561  0.027063  0.059448  0.003079  0.088162
  0.39181:  0.001357  0.004753  0.002328  0.047212  0.190545  0.031137  0.078262
  0.88614:  0.012572  0.029788  0.082503  0.002168  0.033906  0.000366  0.140053
  1.96893:  0.000184  0.001708  0.001732  0.012048  0.088378  0.022026  0.069046
```

This are the dipole matrix elements for the $<T_2 \mid T_1 \mid T_1>$ transition. Its contribution to the spectral shape is given by those transitions from the lowest energy state, i.e. the line with the energy −2.57243. Using the same method as described in chapter 3, one can actually print individually all four triads of the Ni2+ calculation.

The file als5ni2t2.plo plots all four different transition matrix elements, as given below. The file als5ni2t2.plo looks like:

```
postscript als5ni2t2.ps
landscape
energy_range 850 880
columns_per_page 2
rows_per_page 2
frame_title Ni 2pXAS
lorentzian 0.2 999. range 0 860
lorentzian 0.4 999.   range 860 999
gaussian 0.25
frame_title GROUND STATE ALL
old_racah als5ni2.ora
frame_title T2 to T1
spectrum fstate 1-
frame_title T2 to E
spectrum fstate 2-
frame_title T2 to T2
spectrum fstate ^1-
frame_title T2 to A2
spectrum fstate ^0-
end
```

The important command lines are the line old_racah als5ni2.ora, that reads the correct outputfile. The line spectrum fstate 1- calculates the spectral shape with the limitation that only those final states with 1- symmetry (=T1) have been included.

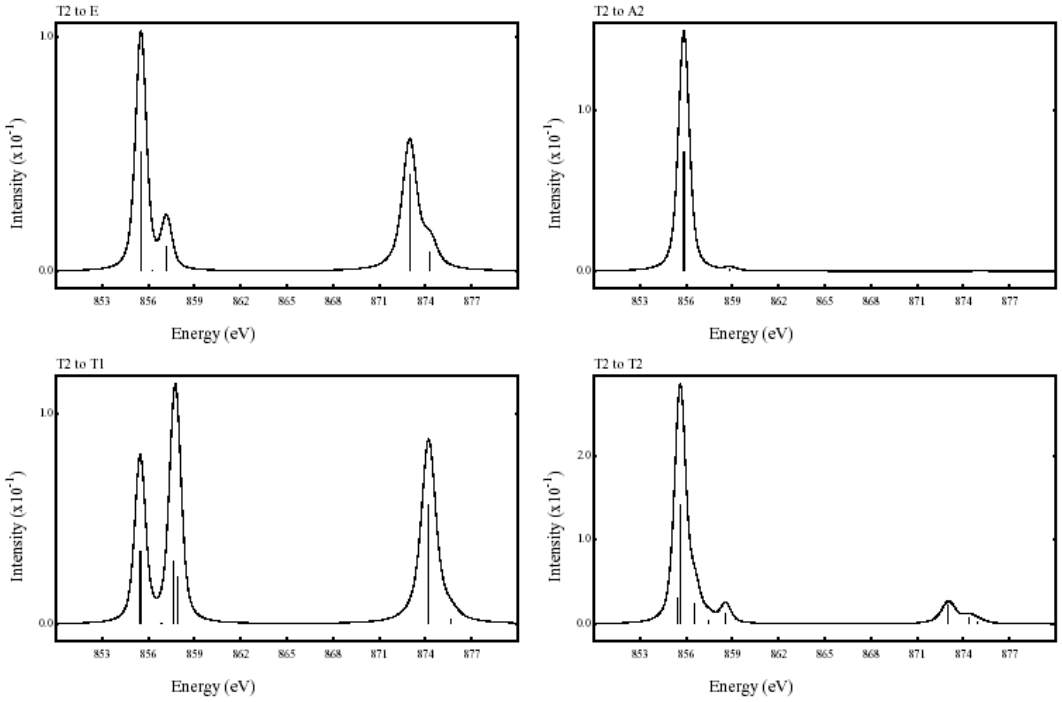

These four figures give the four individual matrix elements for the Ni2+ calculation in octahedral symmetry. In practise, one always observes the addition of these four spectra. It can also be useful to compare the spectrum of the ground state with the spectra of excited states. In the calculation of the TSD we found that the ground state

has T2 symmetry, while four (nearly) degenerate states related to 3T2 symmetry are found at 1.0 eV higher energy. One can plot all these spectra with the file als5ni2g.plo. This file is equivalent to the final state calculation. A difference is the parity of the initial state, which is positive. This implies that one has to give a plus sign to the symmetries, instead of a minus sign, for example spectrum istate 1+. The figure below gives the ground state result for the Ni2+ spectrum, plus three excited states, for respectively T1, E and A2 symmetry, all part of the 3T2 state at 1.12 eV above the 3A2 ground state.

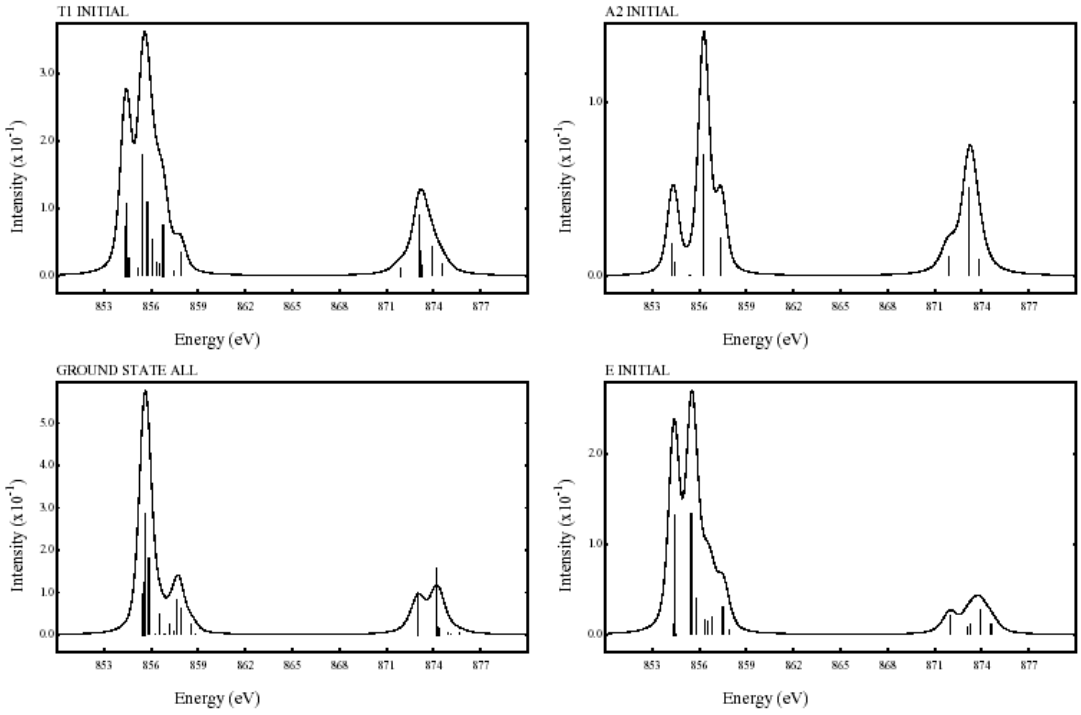

In case of a Ni2+ ion in atomic symmetry, it turned out that the inclusion of 3d spin-orbit coupling was important. Below we compare the atomic results with the crystal field results concerning the inclusion of the 3d spin-orbit coupling. The file als5ni2ls.plo combines the atomic spectra with the crystal field spectra.

The figure below clearly shows that the influence of the 3d spin-orbit coupling is large for a Ni2+ ion in spherical symmetry, while it is small for a Ni2+ ion in cubic symmetry. The reason is that for an atom, the 3F4 ground state is made degenerate with the 3F3 and 3F2 states. In cubic symmetry, the 3A2 ground state is not split by the 3d spin-orbit coupling, and another important factor is that the energy difference to the next state is over 1.0 eV. Although the spectra of cubic Ni2+ look rather similar with and without 3d spin-orbit coupling, they are not identical. One can check this by exporting the data to an external data analysis program (later more how to do this), but the plotting program has also the option to plot spectral differences. The file als5ni2ls2.plo plots the spectrum with 3d spin-orbit coupling (bottom) and also the difference with the spectrum without 3d spin-orbit coupling. A significant difference is observed. With good experimental data quality, one could use these calculations to

check whether the 3d spin-orbit coupling should be switched off or on, for example from the L3 and L2 peak ratios. In other systems, for example Co2+ and Cr4+, the role of the 3d spin-orbit coupling is much more significant, as will be discussed below.

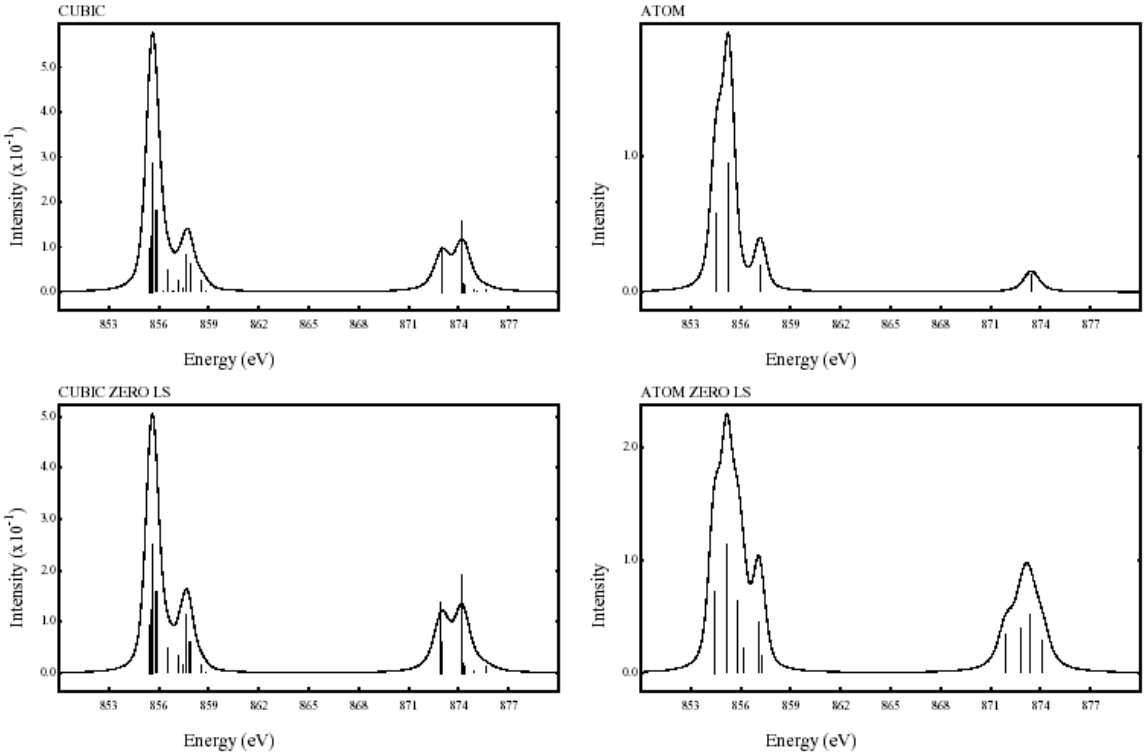

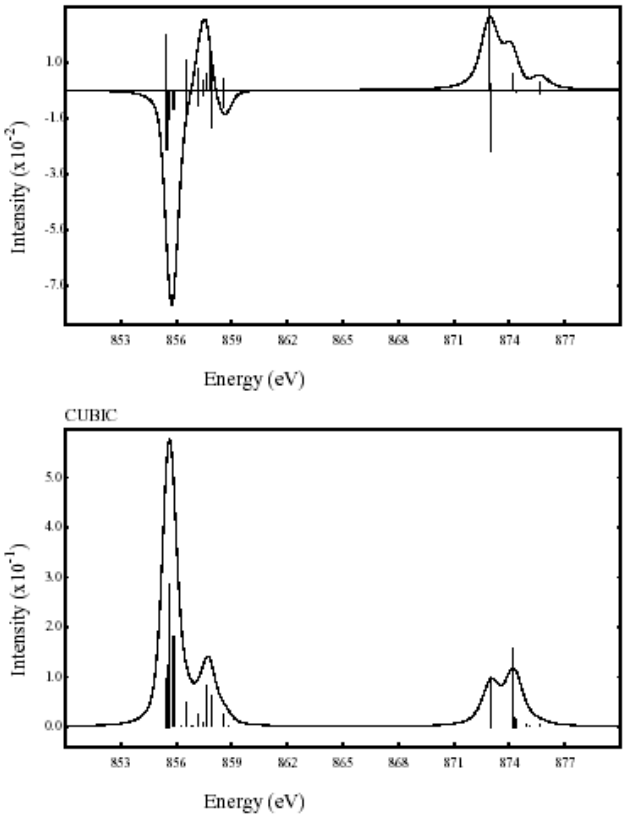
1.0
-1.0
-3.0
-5.0
-7.0
Intensity (x10^{-2})
853
856
859
862
865
868
871
874
877
Energy (eV)
CUBIC
5.0
4.0
3.0
2.0
1.0
0.0
Intensity (x10^{-1})
853
856
859
862
865
868
871
874
877
Energy (eV)

The ground states of $3d^N$ systems

The ground state of a $3d^8$ configuration in O_h symmetry always remains $^3A_2$. The reason is clear if one compares these configurations to the single particle description of a $3d^8$ configuration. In a single particle description a $3d^8$ configuration is split by the cubic crystal field into the t_{2g} and the e_g configuration, following the branching rules from table 3.6. Having found these configurations, one adds the eight 3d electrons one-by-one to these configurations. The t_{2g} configuration has the lowest energy and can contain six 3d electrons. The remaining two electrons are placed in the e_g configuration, where both have a parallel alignment according to Hunds rule. The result is that the overall configuration is $t_{2g}^6 e_g(up)^2$. This configuration identifies with the $^3A_2$ configuration.

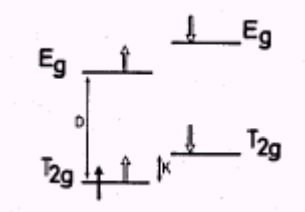

Figure 3.1 The splitting of a single 3d-electron under influence of the cubic crystal field D and the Stoner exchange interaction J. A second electron is indicated with an empty arrow to indicate the energy effects.

Figure 3.3 shows the splitting of a 3d configuration into an e_g and a t_{2g} configuration. Both configurations are further split by the Stoner exchange splitting J. The Stoner exchange splitting J is given as a linear combination of the Slater-Condon parameters as $J=(F_2+F_4)/14$. The Stoner exchange splitting is an approximation to the effects of the Slater-Condon parameters and in fact a second parameter C, the orbital polarisation, can be used in combination with J. The orbital polarisation C is given as $C=(9F_2-5F_4)/98$. Often this orbital polarisation is omitted from single particle descriptions. In that case the multiplet configuration $^3A_2$ is not exactly equal to the single particle configuration $t_{2g}^6 e_g(up)^2$. We assume for the moment that the effect of the orbital polarisation will not modify the ground states. Then one can use figure 3.2 to show that the ground states of $3d^N$ configurations are those as given in table 3.10.

The configurations $3d^0$ to $3d^9$ are given in O_h symmetry for all possible high-spin (HS) and low-spin (LS) states. The third column gives the HS term symbols and the last column the LS term symbols. The fourth and fifth columns give the respective occupations of the t_{2g} and e_g orbitals.

Conf.	Ground State in SO_3	HS Ground State in O_h	HS Ground State in Single particle models	LS Ground State in Single particle models	LS Ground State in O_h
$3d^0$	$^1S_0$	$^1A_1$	-	-	-
$3d^1$	$^2D_{3/2}$	$^2T_2$	t_{2g+}^1	-	-
$3d^2$	$^3F_2$	$^3T_1$	t_{2g+}^2	-	-
$3d^3$	$^4F_{3/2}$	$^4A_2$	t_{2g+}^3	-	-
$3d^4$	$^5D_0$	^5E	$t_{2g+}^3 e_{g+}^1$	$t_{2g+}^3 t_{2g-}^1$	$^3T_1$
$3d^5$	$^6S_{5/2}$	$^6A_1$	$t_{2g+}^3 e_{g+}^2$	$t_{2g+}^3 t_{2g-}^2$	$^2T_2$
$3d^6$	$^5D_2$	$^5T_2$	$t_{2g+}^3 e_{g+}^2 t_{2g-}^1$	$t_{2g+}^3 t_{2g-}^3$	$^1A_1$
$3d^7$	$^4F_{9/2}$	$^4T_1$	$t_{2g+}^3 e_{g+}^2 t_{2g-}^2$	$t_{2g+}^3 t_{2g-}^3 e_{g+}^1$	^2E
$3d^8$	$^3F_4$	$^3A_2$	$t_{2g+}^3 e_{g+}^2 t_{2g-}^3$	-	-
$3d^9$	$^2D_{5/2}$	^2E	$t_{2g+}^3 e_{g+}^2 t_{2g-}^3 e_{g-}^1$	-	-

Table 3.10 shows that for the configurations $3d^4$, $3d^5$, $3d^6$ and $3d^7$ there are two possible ground state configurations in O_h symmetry. A high-spin ground state that originates from the Hunds rule ground state plus a low-spin ground state for which first all t_{2g} levels are filled. One can directly relate the symmetry of a configuration to the partly filled sub-shell in the single particle model. A single particle configuration with one t_{2g} electron has T_2 symmetry, two t_{2g} electrons imply T_1 symmetry and one e_g electron implies E symmetry. If the t_{2g} electrons are filled and the e_g electrons (of the same spin) are empty the symmetry is A_2. Finally, if both the t_{2g} and e_g states (of the same spin) are filled the symmetry is A_1. The nature of the ground state is important, as we will show below that E symmetry states are susceptible to Jahn-Teller distortions and T_1 and T_2 symmetry states are susceptible to the effects of the 3d spin-orbit coupling.

The transition from high-spin top low-spin ground states is determined by the cubic crystal field 10Dq and the exchange splitting J. The exchange splitting is present for every two parallel electrons. Table 3.10 gives the high-spin and low-spin occupations of the t_{2g} and e_g spin-up and spin-down orbitals t_{2g+}, e_{g+}, t_{2g-} and e_{g-}. The $3d^4$ and $3d^7$ configuration differ by one t_{2g} versus e_g electron hence one time the crystal field splitting D. The $3d^5$ and $3d^6$ configurations differ by 2D. The exchange interaction J is slightly different for e_ge_g, e_gt_{2g} and $t_{2g}t_{2g}$ interactions and column 5 of table 3.11 contains the overall exchange interactions. The last column can be used to estimate the transition point. For this column the exchange splittings were assumed to be equal, yielding the simple rules that for $3d^4$ and $3d^5$ configurations high-spin states are found if the crystal field splitting is less than 3J. In case of $3d^6$ and $3d^7$ configurations the crystal field value should be less than 2J for a high-spin configuration. Because J can be estimated as 0.8 eV, the transition points are approximately 2.4 eV for $3d^4$ and $3d^5$, respectively 1.6 eV for $3d^6$ and $3d^7$. In other words $3d^6$ and $3d^7$ materials have a tendency to be low-spin compounds. This is particularly true for $3d^6$ compounds because of the additional stabilising nature of the $3d^6$ $^1A_1$ low spin ground state.

Conf.	High-Spin	Low-Spin	10Dq (D)	Exchange (J)	J/D
$3d^4$	$t_{2g+}^3\, e_{g+}^1$	$t_{2g+}^3\, t_{2g-}^1$	1D	$3J_{te}$	3
$3d^5$	$t_{2g+}^3\, e_{g+}^2$	$t_{2g+}^3\, t_{2g-}^2$	2D	$6J_{te}+J_{ee}-J_{tt}$	~3
$3d^6$	$t_{2g+}^3\, e_{g+}^2\, t_{2g-}^1$	$t_{2g+}^3\, t_{2g-}^3$	2D	$6J_{te}+J_{ee}-3J_{tt}$	~2
$3d^7$	$t_{2g+}^3\, e_{g+}^2\, t_{2g-}^2$	$t_{2g+}^3\, t_{2g-}^3\, e_{g+}^1$	1D	$3J_{te}+J_{ee}-2J_{tt}$	2

Table 3.11 The high-spin and low-spin distribution of the 3d electrons for the configurations $3d^4$ to $3d^7$. The fourth column gives the difference in crystal field energy, the fifth column the difference in exchange energy. For the last column, we have assumed that $J_{te}\sim J_{ee}\sim J_{tt}=J$.

The effect of the 3d spin-orbit coupling

As discussed above the inclusion of 3d spin-orbit coupling will bring one to the multiplication of the spin and orbital moments to a total moment. In this process one loses the familiar nomenclature for the ground states of the $3d^N$ configurations. For example the ground state of Ni^{II} in octahedral symmetry is in total symmetry referred to as T_2 and not as $^3A_2$. In total symmetry also the spin moments are branched to the same symmetry group as the orbital moments, yielding for a $^3A_2$ ground state an overall ground state of $T_1 \otimes A_2 = T_2$. It turns out that in many cases it is better to omit the 3d spin-orbit coupling because it is 'quenched', for example by solid state effects. This has been found to be the case for CrO_2. A different situation is found for CoO, where the explicit inclusion of the 3d spin-orbit coupling is essential for a good description of the 2p x-ray absorption spectral shape. In other words 2p x-ray absorption is able to determine the different role of the 3d spin-orbit coupling in respectively CrO_2 (quenched) and CoO (not quenched).

Table 3.13 gives the spin-projection to O_h symmetry. The ground states with an odd number of 3d electrons do have a ground state spin moment that is half-integer. These half-integer configurations have not been included in the discussion of the character tables discussed above and can be found elsewhere.. Table 3.13 shows that the degeneracy of the overall symmetry states is often not exactly equal to the spin number as given in the third column. For example the $^3T_1$ ground state is split into four configurations, not three as one would expect. If the 3d spin-orbit coupling is small (and if no other state is close in energy), two of these four states are quasi-degenerate and one finds essentially three states. This is in general the case for all situations. Note that the $^6A_1$ ground state of $3d^5$ is split into two configurations. These configurations are degenerate as far as the 3d spin-orbit coupling is concerned. However because of differences in the mixing of excited term symbols a small energy difference can be found. This is the origin of the small but non-zero zero field splitting in the EPR analysis of $3d^5$ compounds.

Conf.	Ground State in SO3	High-Spin Ground State in Oh	Spin in Oh	Deg.	Overall Symmetry in Oh
$3d^0$	$^1S_0$	$^1A_1$	A_1	1	A_1
$3d^1$	$^2D_{3/2}$	$^2T_2$	U_1	2	$U_2 + G$
$3d^2$	$^3F_2$	$^3T_1$	T_1	4	$E+T_1+T_2+A_1$
$3d^3$	$^4F_{3/2}$	$^4A2$	G	1	G
$3d^4$	$^5D_0$	^5E $3T_1$	$E + T_2$ T_1	5 4	$A_1+A_2+E+T_1+T_2$ $E+T_1+T_2+A_1$
$3d^5$	$^6S_{5/2}$	$^6A_1$ $2T_2$	$G+U_2$ U_1	2 2	$G+U_2$ $G+U_2$
$3d^6$	$^5D_2$	$^5T_2$ $1A_1$	$E+T_2$ A_1	6 1	$A_1+E+T_1+T_1+T_2+T_2$ A_1
$3d^7$	$^4F_{9/2}$	$^4T_1$ 2E	G U_1	4 1	$U_1+U_2+G + G$ G
$3d^8$	$^3F_4$	$^3A_2$	T_1	1	T_2
$3d^9$	$^2D_{5/2}$	^2E	U_1	1	G

Table 3.12 The branching of the spin-symmetry states and its consequence on the states that are found after the inclusion of spin-orbit coupling. The fourth column gives the spin-projection and the fifth column its degeneracy. The last column lists all the symmetry states after inclusion of spin-orbit coupling.

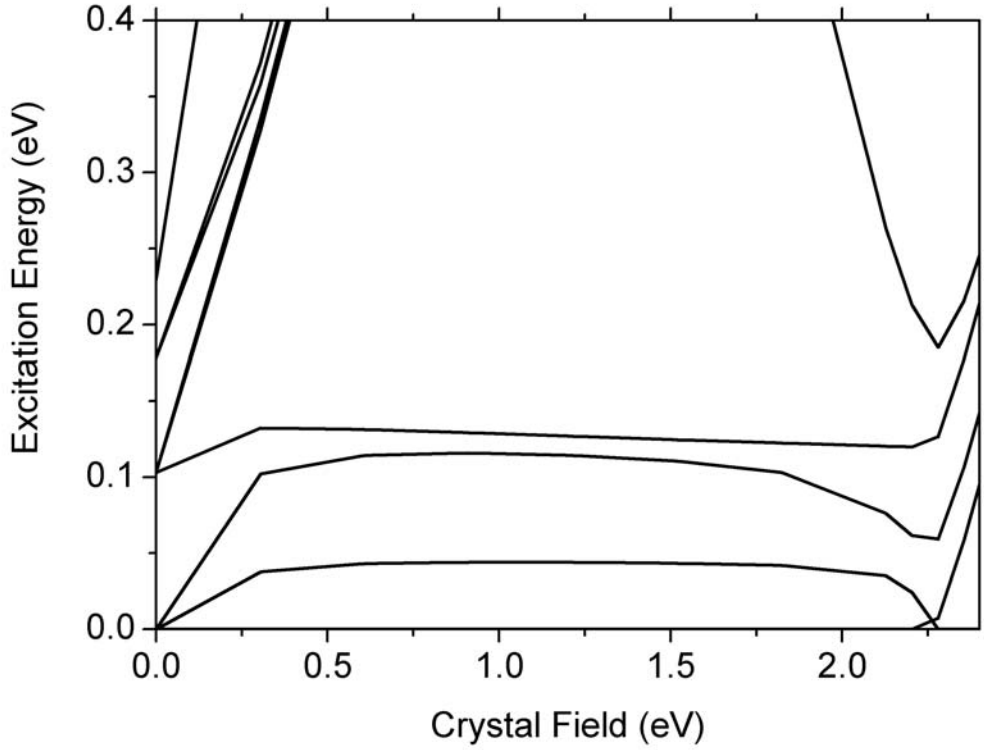

Figure 3.2. The Tanabe-Sugano diagram for a $3d^7$ configuration in O_h symmetry.

Figure 3.4 shows the Tanabe-Sugano diagram for a $3d^7$ configuration in O_h symmetry. Only the excitation energies from 0.0 to 0.4 eV are shown to highlight the high-spin low-spin transition at 2.25 eV and also the important effect of the 3d spin-orbit coupling. It can be observed that the atomic multiplet spectrum of Co^{II} has a large number of states at low energy. All these states are part of the $^4F_{9/2}$ configuration that is split by the 3d spin-orbit coupling. After applying a cubic crystal field, most of these multiplet states are shifted to higher energies and only four states remain at low energy. These are the four states of $^4T_1$ as indicated in table 3.13. These four states all remain within 0.1 eV from the U_1 ground state. That this description is actually correct has been shown in detail for the 2p x-ray absorption spectrum of CoO(de Groot 1991), which has a cubic crystal field of 1.2 eV. At 2.25 eV the high-spin low-spin transition is evident. A new state is coming from high energy and a G-symmetry state replaces the U_1 symmetry state at the lowest energy. In fact there is a very interesting complication: due to the 3d spin-orbit coupling the G-symmetry states of the $^4T_1$ and ^2E configurations mix and form linear combinations. Just above the transition point, this linear combination will have a spin-state that is neither high-spin nor low-spin and in fact a mixed spin-state can be found. (MORE SOON, example of CoO calculation)

Symmetry effects in D_{4h} symmetry

In D_{4h} symmetry the t_{2g} and e_g symmetry states split further into e_g and b_{2g} respectively a_{1g} and b_{1g}. Depending on the nature of the tetragonal distortion either the e_g or the b_{2g} state have the lowest energy. Table 3.12 shows that all configurations from $3d^2$ to $3d^8$ have a low-spin possibility in D_{4h} symmetry. Only the $3d^2$ configuration with the e_g state as ground state does not posses a low-spin configuration. The $3d^1$ and $3d^9$ configurations contain only one unpaired spin thus they have no possibility to obtain a low-spin ground state. It is important to notice that a $3d^8$ configuration as for example found in Ni^{II} and Cu^{III} can yield a low-spin configuration. Actually this low-spin configuration is found in the trivalent parent compounds of the high T_C superconducting oxides(Hu and others 1998). The D_{4h} symmetry ground states are particularly important for those cases where O_h symmetry yields a half-filled e_g state. This is the case for $3d^4$ and $3d^9$ plus low-spin $3d^7$. These ground states are unstable in octahedral symmetry and will relax to, for example, a D_{4h} ground state, the well-known Jahn-Teller distortion. This yields the Cu^{II} ions with all states filled except the $^1A_{1g}$-hole.

General calculation $3d^N \rightarrow 2p^5 3d^{N+1}$ in D_{4h} symmetry		
Initial State	Transition	Final State
$<A_1 \mid A_1 \mid A_1>$	$<A_1 \mid E \mid E>$ $<A_1 \mid A_2 \mid A_2>$	$<A_1 \mid A_1 \mid A_1>$
$<B_1 \mid A_1 \mid B_1>$	$<B_1 \mid E \mid E>$ $<B_1 \mid A_2 \mid B_2>$	$<B_1 \mid A_1 \mid B_1>$
$<E \mid A_1 \mid E>$	$<E \mid E \mid A_1>$ $<E \mid E \mid A_2>$ $<E \mid E \mid B_1>$ $<E \mid E \mid B_2>$ $<E \mid A_2 \mid A_2>$	$<E \mid A_1 \mid E>$
$<B_2 \mid A_1 \mid B_2>$	$<B_2 \mid E \mid E>$ $<B_2 \mid A_2 \mid B_1>$	$<B_2 \mid A_1 \mid B_2>$
$<A_2 \mid A_1 \mid A_2>$	$<A_2 \mid E \mid E>$ $<A_2 \mid A_2 \mid A_1>$	$<A_2 \mid A_1 \mid A_2>$

Table 3.13 The matrix elements in D_{4h} symmetry needed for the calculation of 2p x-ray absorption. Boldface matrix elements apply to a $3d^0$ configuration.

Ground State in Single particle models in D_{4h} symmetry				
Conf.	High-Spin $e_g < b_{2g}$	High-Spin $b_{2g} < e_g$	Low-Spin $e_g < b_{2g}$	Low-Spin $b_{2g} < e_g$
$3d^1$	2 e_{g+}	2 b_{2g+}	-	-
$3d^2$	3 e_{g+}^2	3 b_{2g+} e_{g+}	-	1 b_{2g+} b_{2g-}
$3d^3$	4 $e_{g+}^2 b_{2g+}$	4 b_{2g+} e_{g+}^2	2 e_{g+}^2 e_{g-}	2 b_{2g+} e_{g+} b_{2g-}
$3d^4$	5 e_{g+}^2 $b_{2g+}a_{1g+}$	5 b_{2g+} $e_{g+}^2 b_{1g+}$	1 e_{g+}^2 e_{g-}^2	3 b_{2g+} e_{g+}^2 b_{2g-}
$3d^5$	6 e_{g+}^2 $b_{2g+}a_{1g+}b_{1g+}$	6 $b_{2g+}e_{g+}^2 b_{1g+}a_{1g+}$	2 e_{g+}^2 b_{2g+} e_{g-}^2	2 b_{2g+} e_{g+}^2 b_{2g-} e_{g-}
$3d^6$	5 e_{g+}^2 $b_{2g+}a_{1g+}b_{1g+}$ e_{g-}	5 b_{2g+} $e_{g+}^2 b_{1g+}a_{1g+}$ b_{2g-}	1 e_{g+}^2 b_{2g+} e_{g-}^2 b_{2g-}	1 b_{2g+} e_{g+}^2 b_{2g-} e_{g-}^2
$3d^7$	4 $e_{g+}^2 b_{2g+}a_{1g+}b_{1g+}$ e_{g-}^2	4 $b_{2g+}e_{g+}^2 b_{1g+}$ a_{1g+} $b_{2g-}e_{g-}$	2 e_{g+}^2 b_{2g+} a_{1g+} e_{g-}^2 b_{2g-}	2 b_{2g+} e_{g+}^2 b_{1g+} b_{2g-} e_{g-}^2
$3d^8$	3 e_{g+}^2 $b_{2g+}a_{1g+}b_{1g+}$ e_{g-}^2 b_{2g-}	3 $b_{2g+}e_{g+}^2 b_{1g+}$ a_{1g+} b_{2g-}^1 e_{g-}^2	1 e_{g+}^2 b_{2g+} a_{1g+} e_{g-}^2 b_{2g-} a_{1g-}	1 b_{2g+} e_{g+}^2 b_{1g+} b_{2g-} e_{g-}^2 b_{1g-}
$3d^9$	2 $e_{g+}^2 b_{2g+}a_{1g+}b_{1g+}$ e_{g-}^2 $b_{2g-}a_{1g-}$	2 $b_{2g+}e_{g+}^2 b_{1g+}a_{1g+}$ $b_{2g-}e_{g-}^2 b_{1g-}$	-	-

Table 3.14 The configurations $3d^1$ to $3d^9$ are given in D_{4h} symmetry for all high-spin and low-spin possibilities for the two cases that the e_g energy is lowest and that the b_{2g} energy is lowest. The number in boldface indicates the spin-degeneracy 2S+1 for all configurations.